A Section 508–conformant HTML version of this article is available at https://doi.org/10.1289/EHP5221.

Effects of Benzophenone-3 and Propylparaben on Estrogen Receptor–Dependent R-Loops and DNA Damage in Breast Epithelial Cells and Mice

Prabin Dhangada Majhi,[1,2] Aman Sharma,[1*] Amy L. Roberts,[1] Elizabeth Daniele,[1] Aliza R. Majewski,[1] Lynn M. Chuong,[1] Amye L. Black,[1] Laura N. Vandenberg,[4] Sallie S. Schneider,[3,5] Karen A. Dunphy,[1] and D. Joseph Jerry[1,5]*

[1]Department of Veterinary & Animal Sciences, University of Massachusetts, Amherst, Massachusetts, USA
[2]Department of Botany, Ravenshaw University, Cuttack, Odisha, India
[3]University of Massachusetts Medical School, Baystate Campus, Springfield, Massachusetts, USA
[4]Department of Environmental Health Sciences, University of Massachusetts, Amherst, Massachusetts, USA
[5]Pioneer Valley Life Sciences Institute, Springfield, Massachusetts, USA

Background: Endocrine-disrupting chemicals have been shown to have broad effects on development, but their mutagenic actions that can lead to cancer have been less clearly demonstrated. Physiological levels of estrogen have been shown to stimulate DNA damage in breast epithelial cells through mechanisms mediated by estrogen-receptor alpha (ERα). Benzophenone-3 (BP-3) and propylparaben (PP) are xenoestrogens found in the urine of >96% of U.S. population.

Objectives: We investigated the effect of BP-3 and PP on estrogen receptor–dependent transactivation and DNA damage at concentrations relevant to exposures in humans.

Methods: In human breast epithelial cells, DNA damage following treatment with 17β-estradiol (E_2), BP-3, and PP was determined by immunostaining with antibodies against γ-H2AX and 53BP1. Estrogenic responses were determined using luciferase reporter assays and gene expression. Formation of R-loops was determined with DNA: RNA hybrid–specific S9.6 antibody. Short-term exposure to the chemicals was also studied in ovariectomized mice. Immunostaining of mouse mammary epithelium was performed to quantify R-loops and DNA damage *in vivo*.

Results: Concentrations of 1 μM and 5 μM BP-3 or PP increased DNA damage similar to that of E_2 treatment in a ERα-dependent manner. However, BP-3 and PP had limited transactivation of target genes at 1 μM and 5 μM concentrations. BP-3 and PP exposure caused R-loop formation in a normal human breast epithelial cell line when ERα was introduced. R-loops and DNA damage were also detected in mammary epithelial cells of mice treated with BP-3 and PP.

Conclusions: Acute exposure to xenoestrogens (PP and BP-3) in mice induce DNA damage mediated by formation of ERα-dependent R-loops at concentrations 10-fold lower than those required for transactivation. Exposure to these xenoestrogens may cause deleterious estrogenic responses, such as DNA damage, in susceptible individuals. https://doi.org/10.1289/EHP5221

Introduction

Endocrine-disrupting chemicals (EDCs) alter the endocrine system by binding directly to the receptors and modulating downstream signaling pathways. Xenoestrogens are structurally diverse EDCs that affect estrogen receptor (ER) signaling pathways. BP-3 (oxybenzone, or 2-Hydroxy-4-methoxybenzophenone, CAS No. 131-57-7) is a UV-filter used in personal care products, such as sunscreens, cosmetics, and lotions, with concentrations up to 0.148% (Liao and Kannan 2014) and a maximum allowed concentration of 6% by Food and Drug Administration (FDA) and European commission (EC 2017). BP-3 was detected in the urine samples of 96.8% of U.S. population in the 2003–2004 National Health and Nutrition Examination Survey (NHANES) conducted by the Centers for Disease Control and Prevention (CDC) (Calafat et al. 2008). Similarly, PP (propyl parahydroxybenzoate, CAS No. 94-13-3) is widely used as an antimicrobial agent in food and personal care products. Although the FDA limits PP to 0.1% in food, currently there is no specific limit for preservatives in personal care products. PP is banned as a food preservative, and maximum permissible levels in personal care products is 0.4% in the European Union (EU) (Snodin 2017; EC 2014). PP was detected in the urine samples of >96% of U.S. population surveyed during 2003–2005 by the CDC (Ye et al. 2006).

Estrogenic responses are determined by the action of two distinct estrogen receptor (ER) subtypes, estrogen receptor α (ERα) and estrogen receptor β (ERβ). Ligand-activated ER recruits coactivators to estrogen response elements (ERE) in promoters of target genes leading to transcription initiation (Shang et al. 2000; Yi et al. 2017). In ERα expressing breast cancer cells, proliferation is among the types of cellular responses (Henderson et al. 1988; Musgrove and Sutherland 1994). Hence, estrogenic responses to putative xenoestrogens is most often determined by transactivation of ERE-reporters, endogenous gene expression and cell proliferation in ER-expressing MCF-7 and T47D cell lines, where ERα is the dominant subtype (Buteau-Lozano et al. 2002; Vladusic et al. 2000). These studies showed BP-3 was a weak agonist of ER at 1 μM (Kerdivel et al. 2013; Schlotz et al. 2017; Schlumpf et al. 2001). BP-3 was found in the urine samples of 25 volunteers who used sunscreen containing 4% BP-3 twice a day for 5 d, suggesting it was readily absorbed through skin (Gonzalez et al. 2006). Metabolites of BP-3, such as 2,4-diOH-BP and 2,3,4-triOH BP, were shown to form by oxidation in rat and human liver microsomes (Okereke et al. 1994; Watanabe et al. 2015). 2,4-diOH-BP was detected in the urine samples of women scheduled to undergo a diagnostic and/or

*Both authors contributed equally to this work.
Address correspondence to D. Joseph Jerry, Department of Veterinary & Animal Sciences, University of Massachusetts, 661 North Pleasant St., Integrated Life Sciences Building, Amherst, MA 01003, USA; Pioneer Valley Life Sciences Institute, 3601 Main St., Springfield, MA 01199, USA. Telephone: (413) 545-5335. Email: Jjerry@vasci.umass.edu

Supplemental Material is available online (https://doi.org/10.1289/EHP5221).
L.N.V. has received funding from the Cornell Douglas Foundation and Paul G. Allen Foundation. She has been reimbursed for travel expenses by several organizations, including SweTox, the European Commission, the Mexican Endocrine Society, Advancing Green Chemistry, CropLife America, Beautycounter (Counter Brands, LLC), and many universities, to speak about endocrine disruptors. All other authors declare they have no actual or potential competing financial interests.
Received 20 February 2019; Revised 13 November 2019; Accepted 19 November 2019; Published 15 January 2020.

therapeutic laparoscopy or laparotomy as part of the ENDO study (Kunisue et al. 2012) and was shown to have higher ER transactivation potential in comparison with BP-3 (Watanabe et al. 2015). BP-3 and BP-3 metabolite 4,4′-dihydroxybenzophenone were also detected in 27 of the 79 breast milk samples from mothers who had normal pregnancy and delivery, and who participated in the Breast Milk Bank of the Blood and Tissue Bank of Catalonia (Spain) (Molins-Delgado et al. 2018). Exposure of BP-3 during pregnancy and lactation in mice resulted in altered mammary gland ductal architecture that persisted for weeks after exposures ended (LaPlante et al. 2018). Long-term exposure of MCF-7 breast cancer cells to 100 μM BP-3 for >20 weeks increased the motility of these cells (Alamer and Darbre 2018). This increase was also observed in estrogen nonresponsive cell line MDA-MB-231, suggesting alternate pathways of BP-3 actions at this dose. Similarly, PP was shown to be an effective ER-agonist with 1.3-fold induction of gene expression using reporter assays (ERE-CAT reporter) at 10 μM, increased expression of estrogen-responsive gene Trefoil Factor 1 (*TFF1*, also known as pS2) and increased proliferation of MCF-7 cells at 1 μM (Byford et al. 2002). Proliferation induced by PP was inhibited by ER antagonist (fulvestrant) indicating dependence on ERα. PP also increased cell motility (increased scratch closure) in both short-term (7-d) and long-term (20-wk) treatments in the MCF-7 cell line (Khanna et al. 2014).

In addition to stimulating cell proliferation and motility, estrogen also induces genotoxicity and DNA damage and is considered a major risk factor in breast cancer etiology (Roy and Liehr 1999; Yager and Davidson 2006). Estrogen has been shown to induce DNA damage by *a*) metabolic activation of estrogen and *b*) hormonal carcinogenesis (Santen et al. 2009). E_2 is metabolized to form catechol estrogens (16α-OHE_2 or 2-OHE_2 and 4-OHE_2), which can be oxidized to form reactive semiquinone (SQ) intermediates and quinone derivatives. Two such compounds, E_2-3-4-Q and E_2-2-3-Q form stable DNA adducts or depurinating adducts, such as 4-OHE_2-1-N7Gua and 4-OHE_2-1-N3Ade, which were associated with increased breast cancer risk, but micromolar levels of E_2-3-4-Q and E_2-2-3-Q were required to show DNA adduct formation *in vitro* (Cavalieri and Rogan 2016). The SQ and quinone derivatives can also generate ROS through redox cycling, which can be genotoxic (Fussell et al. 2011; Wang et al. 2010). Similarly, ER–independent DNA damage was shown in ERα-negative cell lines using the COMET assay (Rajapakse et al. 2005), *cII* mutagenesis assay (Zhao et al. 2006), or LOH (Huang et al. 2007; Russo et al. 2003). The concentrations of E_2 or 4-OHE_2 used in these studies were ≥70 nM, with the exception of Russo et al. 2003, who reported increased clonal efficiency of MCF10F cells at 0.007 nM. However, the median E_2 level during pregnancy is 74 nM and <2 nM in normal cycling women (Table 1), and the level of circulating estradiol metabolites are 100-fold lower (Xu et al. 2007; Ziegler et al. 2010). Clinical data show that in postmenopausal women with ER-positive early breast cancer, endocrine therapy with an aromatase inhibitor was associated with significantly lower recurrence than tamoxifen (TAM) therapy (EBCTCG 2015), which could be because of either lower levels of estrogen metabolites or reduced ER activation. Epidemiological data show that for a given level of total estrogen, increased levels of 4-OHE_2, 2-OHE_2 and 16-OHE_2 are associated with reduced risk in breast cancer (Dallal et al. 2014; Moore et al. 2016; Sampson et al. 2017) or no independent association with risk (Sampson et al. 2017); however, an earlier study reported 4-OHE_2 levels to be associated with higher breast cancer risk (Fuhrman et al. 2012). Hence, the impact of metabolic activation of estrogen at physiologically relevant concentrations on DNA damage remains to be demonstrated.

Hormonal carcinogenesis is postulated to act through ER to initiate lesions as well as stimulate progression of tumors. E_2 treatment stimulated renal tumors in male Syrian hamsters (Liehr et al. 1988). TAM reduced tumors but did not alter levels of DNA-adducts, suggesting the primary effect of E_2 being mediated by ER. Similarly, blockage of ER activation through selective estrogen receptor modulators (SERMs), such as TAM and raloxifene, reduced the incidence of breast cancer by 50%–75% in women (Cummings et al. 1999; Cuzick and International Breast Cancer Intervention Study 2001; Martino et al. 2004). Bilateral oophorectomy and hysterectomy in women under 40 years of age reduced breast cancer later in life by 75% (Feinleib 1968). Administration of aromatase inhibitor (exemestane) for 35 months to a cohort of postmenopausal women with Gail score of 1.66 and prior atypical ductal/lobular hyperplasia or ductal carcinoma *in situ* treated with mastectomy but noncarriers for BRCA1/2 and no prior invasive ductal carcinoma resulted in 65% relative reduction of breast cancer (Goss et al. 2011). Mobley and Brueggemeier showed that 8-oxo-dG production with buthionine sulfoximine (BSO), E_2 (10 nM) and H2O2 treatment could be reduced with TAM treatment in ER-positive MCF7 cells but not in ER-negative MDA-MB-231 cells, suggesting DNA damage was at least partially ER-mediated (Mobley and Brueggemeier 2004). Stork et al. showed lack of DNA damage marker γ-H2AX (phosphorylated H2AX) in MCF10A cells following treatment of 10 nM and 100 nM E_2 for 24 h (Stork et al. 2016). In T47D cells, E_2-mediated γ-H2AX was diminished with treatment of ER inhibitors like TAM or fulvestrant (Periyasamy et al. 2015). ER signaling stimulates proliferation, which was causally linked to tumorigenesis, by increasing the probability of replication errors, which are propagated in daughter cells (Henderson and Feigelson 2000; Preston-Martin et al. 1990). Therefore, E_2 can

Table 1. Estimation of estrogen and xenoestrogens concentrations of estradiol (E_2), benzophenone-3 (BP-3), or propylparaben (PP) in urine/blood samples of women and female mice.

Ligand	Median (μM)	90th or 95th percentile (μM)	Relative transactivation activity at 90th or 95th percentile (% RTA vs. E_2)	References
BP-3 (urine)				
Non-Pregnant	0.137	6.70[b]	18.91 ± 6.62%	Woodruff et al. 2011
Pregnant	0.47	29.5[b]	27.16 ± 6.2%	Philippat et al. 2013
PP (urine)				
Non-Pregnant	0.161	1.98[b]	64.27 ± 20.5%	Calafat et al. 2010
Pregnant	0.253	3.26[b]	104.07 ± 20.98%	Philippat et al. 2013
E_2 (blood)				
Human				
Ovulatory	0.0003–0.0018			Clarke et al. 1997
Luteal	0.0002–0.0008			O'Leary et al. 1991
Pregnant	0.074	0.118[a]		Schock et al. 2016
Mouse	<0.0003			Majewski et al. 2018

[a]90th percentile of exposure in the given population.
[b]95th percentile of exposure in the given population.

be considered as a carcinogen through its actions on progression of cancer that was initiated by other factors.

The studies involving DNA damage by E_2 have used different cell lines, tissues, and end points. Therefore, there is no consistent way to discriminate the contribution of ER-dependent and ER-independent mechanisms across published studies. It is possible that both mechanisms contribute to E_2-mediated carcinogenesis.

Recent studies have shown that ER stimulation leads to transcription-coupled DNA damage, suggesting a distinct mechanism. Interaction of ERα with chromatin forms transcriptional coactivator/corepressor complexes to initiate transcription (Chao et al. 2002; Fullwood et al. 2009; Shang et al. 2000). The open chromatin in these ERα complexes were susceptible to DNA damage by formation of RNA:DNA triplex structures, called R-loops (Stork et al. 2016). Therefore, estrogen can stimulate carcinogenesis by initiating direct DNA damage mediated by ERα and proliferation that expands the population of breast cells.

Bioassays of transcriptional activities have been valuable in rapidly assessing the risk posed by xenoestrogens. However, it is unclear whether the transcriptional activities of xenoestrogens reflect their potential mutagenic activity mediated by ERα. DNA damage by selective ERα agonists such as diethylstilbestrol (DES) and 4,4′,4′′-(4-Propyl-[1*H*]-pyrazole-1,3,5-triyl) *tris*phenol (PPT) (Periyasamy et al. 2015) suggest that transcriptional DNA damage needs to be assessed to determine potential breast cancer risk posed by xenoestrogens. In this study, we evaluated effects of two xenoestrogens, BP-3 and PP, which differ in structure and transcriptional potency and compared these with E_2.

Methods

Cell Culture

T47D (ATCC #HTB-133), T47DKBluc (ATCC #CRL-2865) and MCF-7 (ATCC #HTB 22) cells were passaged in growth media containing phenol red–free (PRF) DMEM-F12 (Sigma #D6434) or MEM 1X (Gibco #51200-038) with 10% heat-inactivated FBS (Omega Scientific #FB-02) and 10 μg/ml insulin (Sigma #9278), 2 mM L-glutamine (Hyclone #SH30034.01), gentamycin 15 μg/ml (Gibco #15750-060), and 1X antibiotics/antimycotics (AB/AM, Gibco #15240-062) and incubated at 37°C with 5% CO_2. For experiments, cells were grown in clearing media with charcoal-stripped serum (CSS) (MEM 1x with 10% charcoal dextran–treated FBS (Omega Scientific #FB-04), 10 μg/ml insulin, and 2 mM L-glutamine) for 24–72 h before being plated for experiments.

The 76N-Tert cell line, a human mammary epithelial cell line immortalized with expression of human telomerase reverse transcriptase (TERT), was a gift from Dr. Vimla Band (Zhao et al. 2010). These cells were grown in F-media [250 mL DMEM (-pyruvate) (Gibco #11965-092), 250 mL Ham's F12 (Gibco #11765-054), 5% FBS, 250 ng/mL hydrocortisone (Sigma #H4001), 10 ng/mL human epidermal growth factor (Tonbo Biosciences #21-8356-U100), 8.6 ng/mL cholera toxin vibrio (Millipore Sigma #227035), 1 μg/mL human insulin solution, and 1X antibiotic/antimycotic] and passaged every 2–3 d.

Generation of 76N-Tert-ESR1 Cells

An inducible ERα (*ESR1*) construct was generated using the pINDUCER14 vector (Meerbrey et al. 2011). Specifically, FLAG tag sequence was amplified from pFLAG-CMV-2 (Andersson et al. 1989) using forward primer 5′-ATACCGGTACCATGGACTACAAAGACGATGACGAC-3′ and reverse primer 5′-TCGACCGGTACGCGTGCGATCGCTGAATTCGCGGCAAG-3′. The amplified FLAG sequence was then cleaned using the Monarch PCR & DNA Cleanup Kit (NEB #T1030) and ligated into pINDUCER14 by digesting both plasmids with *AgeI*, performing dephosphorylation with shrimp alkaline phosphatase (NEB #M0371S) and gel electrophoresis and extracting from agarose gel (DNAland Scientific #GP1001). Sequencing of pINDUCER14-FLAG confirmed that the FLAG sequence was inserted.

ESR1 was amplified from a plasmid expressing *ESR1* made in our lab (pIRES-hrGFPII-ESR1, unpublished data). pIRES-hrGFPII-ESR1 contained the *ESR1* cDNA sequence (Open Biosystems #MHS6278-211691051) in the multiple cloning site of the pIRES-hrGFPII vector (Stratagene #240157). *ESR1* was amplified from pIRES-hrGFPII-ESR1 using forward primer 5′-GCAGAAATGACCATGACCCTCCACACCAAAGC-3′ and reverse primer 5′- TAAACGCGTTCAGACCGTGGCAGGGAAACCCT-3′. Ligation of *ESR1* into pINDUCER14-FLAG was done by digesting both plasmids with *EcoRI* and *MluI* and then performing dephosphorylation, cleanup, and extraction as described above. Two linker sequences (Linker A: 5′-AATTGCGCGATCGCGG-3′ and Linker B: 5′-AATTCCGCGATCGCGC-3′) between FLAG and *ESR1* were added to keep the *ESR1* sequence in frame. Sequencing of this final pINDUCER14-FLAG-*ESR1* confirmed that all inserts were in the correct orientation relative to the vector, both FLAG and *ESR1* were in frame, and the *ESR1* sequence was identical to the *Homo sapiens ESR1* gene (Sequencing Primers: F: 5′-CGGTGGGAGGCCTATATAAG-3′, M: 5′-GCTACCATTATGGAGTCTGG-3′, and R: 5′-ACTTATATACGGTTCTCCCC-3′). This final construct was referred to as pIND-*ESR1* and expressed a constitutive GFP reporter as well as ERα with N-terminal FLAG tag.

In addition, 293T cells were cultured in DMEM:F12 (Sigma #D8900) supplemented with 10% FBS, 15 μg/mL gentamycin (Gibco #15750-060), and 1x antibiotic/antimycotic. Cells were lifted with 0.05% trypsin and plated in 60-mm tissue culture dishes at 2.5×10^6 cells per dish for next-day use. 293T cells were then transfected with 3.5 μg pIND-*ESR1*, 3 μg psPAX2 (Addgene #12260) (gag, pol, and rev packaging vector), and 2 μg pMD2.G (Addgene #12259) (vsv-g packaging vector) in antibiotic-free media using Lipofectamine 2000 (Thermo Fisher Scientific). Media was refreshed after 24 h, and viral media was collected at 48 and 54 h post initial transfection. Viral media from transfected 293T was filtered using a 0.45 μM filter (Corning #431220) and added to 76N-Tert cells twice, 6 h apart, in a 1:1 ratio with F-media. After 24 h, viral media was removed and replaced with F-media. Following cell expansion, the cells were pooled and resuspended in 1% FBS in PBS. Selection of the stably transduced cells was performed by FACS for GFP-positive cells using FACSAria II (Becton-Dickinson). 76N-Tert uninfected cells were used as a control to set the background fluorescence. Approximately 5% cells were GFP-positive, suggesting pIND-*ESR1* expression. The GFP-positive cells were collected to 90% purity. These cells were expanded and referred to as 76N-Tert-*ESR1*.

Luciferase Reporter Assay

T47DKBluc cells were grown in clearing media for 72 h and plated in a 24-well plate at 10×10^5 cells/well density. After 24 h, cells were treated with 10 nM E_2 (17β-estradiol, Sigma #E2758), 10 nM fulvestrant (F, ICI 182, 780, Tocris #1047), 0.5 to 50 μM BP-3 (Sigma #H36206) or 0.5 to 50 μM PP (Sigma #P53357). Stock solutions were prepared in DMSO (Sigma #D8418), then diluted to working concentrations in media. Luciferase assays were performed using the Promega Dual-Luciferase Reporter Assay (Promega #E1910). Cells were lysed in 1X Passive Lysis Buffer after treatment for 24 h and then stored at –20°C. Luciferase activity was determined in lysates by using the Polar Star OPTIMA plate reader (BMG Labtech) and expressed in relative light units (RLU). Treatments were compared with 10 nM E_2 included on the plate, and relative

transactivation activity (RTA) is defined as percent transactivation in comparison with 10 nM E_2.

RT-qPCR

RNA from T47D cells, MCF-7 cells, or flash-frozen fourth mammary gland was isolated with TRIzol (ThermoFisher Scientific #15596018) and Direct-zol RNA MiniPrep Plus (Zymo Research #R2072). cDNA was prepared from 1 μL of RNA in 20 μL reaction mix with Protoscript II First Strand cDNA Synthesis Kit (New England Biolabs #E6560S), following the standard protocol provided by the manufacturer. qPCR for *TFF1*, progesterone receptor (*PGR/Pgr*), and Amphiregulin (*AREG/Areg*) was performed using primers in Table S1 (Integrated DNA Technology) and iTaq Universal SYBR Green Supermix (Biorad, #1725121) on CFX96 Real-Time System thermocycler (Bio-Rad). Each run (96-well qPCR plate) included an inter-run calibrator to normalize across experiments. No housekeeping gene was included in the experiment to avoid possible variation due to treatments. Results represent average of three experiments. Data was analyzed with ΔΔCt method, and relative fold change in expression of target gene was compared among control and treatments.

Cell Proliferation Assay

T47D cells grown in clearing media for 72 h was plated as 100 μl of cells suspension having 5,000 or 10,000 cells per well on five 96-well plates (one for each day). The 96-well plate had 12 cell-free wells for a blank and 7 wells per treatment on each plate. After 24 h, media was changed in appropriate wells on each plate to reach the desired final concentration of E_2 (0.5 nM), BP-3 (5, 50 μM) or PP (1, 10 μM) in the given wells. All plates were maintained in a 37°C, 5% CO_2 incubator until media were exchanged, on one plate per day, for 10% Alamar Blue in plating media. Plates were read at the same time each day at 4 h and 8 h after media exchange on a BioTek Synergy 2 plate reader (BioTek) at 570 nm and 600 nm. Percent Alamar Blue reduction was calculated as per the Alamar Blue protocol:

$$\text{Percent reduced} = \frac{(117{,}216 \times \text{test well } A_{570}) - (80{,}586 \times \text{test well } A_{600})}{[155{,}677 \times \text{mean (negative control well } A_{600})] - [14{,}652 \times \text{mean (negative control well } A_{570})]} \times 100$$

Immunostaining

T47D, MCF7, 76N-Tert, or 76N-Tert-*ESR1* cells were grown in clearing media for 48 h and plated on 20 mm glass uncoated coverslips in 12-well plates with a density of 2×10^5 cells/well. After 24 h of growth, cells were treated with 10 nM E_2, 1 or 5 μM BP-3, and 1 or 5 μM PP with or without 1 μM fulvestrant for 24 h. For γ-H2AX/53BP1/ERα, cells were fixed in ice-cold methanol (100%) for 10 min and quenched with 0.1 M glycine for 15 min. Cells were washed with 1X PBS, blocked in 2% BSA/PBS with 0.1% Triton-X 100 for 1 h at room temperature (RT), incubated overnight with anti-γ-H2AX antibody (Cell Signaling #9718S), anti-ERα antibody (Santa Cruz Biotechnology #sc-8002) or anti-53BP1 antibody (Abcam #ab36823) at 4°C, followed by 1 h with anti-rabbit AlexaFluoro 488–conjugated secondary antibody (Cell Signaling #8889S) or anti-mouse AlexaFluoro 488–conjugated (Cell Signaling #4408S) at RT. For S9.6, cells were fixed in ice-cold 100% methanol for 10 min at –20°C, permeabilized in 100% acetone for 1 min at RT, blocked for 30 min in saline sodium citrate pH 7 (SSC, 4X), 3% BSA, and 0.1% Triton-X and incubated with S9.6 antibody (Kerafast #ENH001) for 2 h at RT, followed by 1 h with anti-mouse AlexaFluoro 596–conjugated secondary antibody (Life Technologies #A11062) or antimouse AlexaFluoro 488–conjugated (Cell Signaling #4408S). For each treatment, two replicates of slides were stained with one set of replicates treated with RNase H (NEB #M0297L) for 4 hr at 37°C prior to incubation with primary antibody. Stained cells were mounted with Vectashield mounting medium containing DAPI (Vector Laboratories #H-1,200). Slides were imaged at 60X (immersion oil) with Nikon A1 spectral confocal microscope. Analysis of γ-H2AX and S9.6 intensity per nucleus or foci per nucleus was calculated using Nikon analysis software, where DAPI was used as a mask for the nucleus.

Western Blot

Cells from MCF7 grown in growth media, 76N-Tert (parental), 76N-Tert-*ESR1*, and 76N-Tert-*ESR1* grown in F-media treated with doxycycline for 24 h and 76N-Tert-*ESR1* treated with doxycycline and 10 nM E_2 for 24 h were lysed with ice-cold RIPA lysis buffer [50 mM Tris–HCl, pH 8.0; 150 mM NaCl; 1 mM EDTA; 1% Triton X-100; 1% Sodium deoxycholate; 0.1% SDS; 1% protease inhibitors (Sigma-Aldrich #P8340), 1% phosphatase inhibitor #2 (Sigma-Aldrich #P5726), and 1% phosphatase inhibitor #3 (Sigma-Aldrich #P0044)]. Homogenate was centrifuged at 13,000 rpm for 15 min at 4°C to remove cellular debris. Protein quantification was performed using BCA protein assay (Thermo Scientific #23225). Equal amounts of protein (28 μg) were separated by SDS-PAGE on 10% acrylamide under denaturating conditions and then blotted onto PVDF membrane (Millipore #IPVH00010). Nonspecific binding was blocked with 5% nonfat dry milk in TBST (Tris-buffered saline and Tween® 20 containing 10 mM Tris-HCl, pH 7.5; 150 mM NaCl; 0.05% Tween® 20) for 1 h. The blot was incubated with 1:100 anti-ERα antibody (Abcam #ab16660) overnight at 4°C. After incubation, the blot was washed with TBST and then incubated with HRP-conjugated secondary antibody (1:5000, GE Healthcare #NA934V) for 1 h. Bands were detected using enhanced chemiluminescence solution and visualized using G-box imaging system (Syngene). The blot was washed with TBST and incubated with anti-β actin antibody (1:5000, Sigma #A1978) overnight at 4°C. After washing with TBST and HRP secondary antibody incubation for 1 h (1:5,000, GE Healthcare #NA931C), bands were detected with enhanced chemiluminescence and G-box system. Expected molecular weights were 67 kDa (ERα) and 42 kDa (β actin).

Animal Treatment

Forty mature BALB/c female mice (8 wk old) were purchased from Jackson Laboratory and housed in temperature-controlled facilities with a set temperature of 17.8–26.11°C and humidity of 30%–70%, 12-h alternating day/night light cycle and fed LabChow 5058 ad libitum. All procedures were in accordance with the national guidelines for the care and use of animals and approved by the University of Massachusetts Amherst's Institutional Animal Care and Use Committee.

The mice were ovariectomized before treatment. Briefly, each mouse was anesthetized with a mix of isoflurane and oxygen. The flanks were shaved, sterilized with povidone-iodine (Betadine) and cleaned with alcohol. An incision was made to the skin on the right flank. The underlying muscle layer was nicked to reveal a small hole through which the ovary was pulled out by grasping the periovarian fat. A Serrefine clamp was used to hold the ovary. After ensuring that the blood vessels were constricted to prevent breeding, the ovary was cut from the uterine horn. The periovarian fat was restored into the

peritoneum. The peritoneum was closed with one or two stiches and the skin was closed with 9-mm wound clips. The procedure was repeated on the contralateral side. The mouse was monitored for a week post procedure, and wound clips were removed after 10 d. After 1 wk of recovery, the mice were randomized to four groups and began an acute oral treatment via pipette with vehicle control (tocopherol-stripped corn oil) ($n=7$) or one of three different compounds E_2 ($n=8$), BP-3 ($n=12$), and PP ($n=12$) for 4 d. Each mouse was administered 1 μL of oil per gram of body weight to deliver 250 μg/kg/d E_2, 3,000 μg/kg/d BP-3, or 10,000 μg/kg/d PP or vehicle control. For BP-3 and PP, these doses represent the toxicologically no-adverse-effect-level (NOAEL) doses for each compound based on development and reproductive toxicity assays (Scientific Committee on Consumer Products 2005, 2008; Soni et al. 2001).

Six hours prior to sacrifice, all of the mice were treated with a 5-gray (Gy) dose of gamma radiation. Then 2 h before sacrifice, all mice were injected intraperitoneally with 70 μg/g body weight of BrdU (Sigma Aldrich; Cat. #B5002) that was previously prepared at 10 mg/ml in PBS and filter sterilized. The mice were sacrificed using carbon dioxide followed by cervical dislocation. Whole blood was collected by cardiac puncture and tissues were harvested. One of the fourth mammary gland was fixed in 10% NBF and transferred to 70% alcohol prior to paraffin embedding. The other fourth mammary gland was cleared of lymph node and stored in –70°C. The whole blood was allowed to coagulate at RT for 20 min and then spun down at 2000 × *g* for 10 min at 4°C to retrieve the serum.

Immunostaining of Mouse Mammary Gland

Freshly cut 4-μM paraffin-embedded sections were deparaffinized/rehydrated with 100% xylenes 3 times for 5 min each, 2 times with 100% ethanol for 5 min each, 95% ethanol for 3 min, and 70% ethanol for 3 min. Samples were rinsed with PBS. Antigen unmasking was performed by boiling the samples in 1 mM EDTA for 1 hr. Samples were cooled down to RT and then treated with SSC 0.2X with gentle shaking at RT for 20 min. Samples were blocked in 3% BSA in PBS with 0.5% Tween® 20 for 1 h at RT. Primary antibody incubation was done with monoclonal S9.6 antibody (Kerafast #ENH001) or anti-H2AX antibody (Cell Signaling #9718S) for overnight at 4°C. After primary incubation, samples were washed 3 times with PBS containing 0.5% Tween® 20 and then incubated with anti-mouse AlexaFluoro 488–conjugated (Cell Signaling #4408S) or anti-rabbit AlexaFluoro 488–conjugated secondary antibody (Cell Signaling #8889S) for 1 h at RT. Samples were washed 2 times with PBS containing 0.5% Tween® 20 and 2 times with PBS and then mounted with Vectashield mounting medium containing DAPI. Slides were imaged at 60× with Nikon A1 spectral confocal microscope. Analysis of S9.6 intensity per nucleus or foci per nucleus were calculated using Nikon analysis software, where DAPI was used as a mask for the nucleus. IHC for Ki67 was performed on a DakoCytomation autostainer using 1:1,000 D2H10 primary antibody (cell signaling #9027T) and the Envision HRP detection system (Dako). Positive cells were counted using ImageJ software. A total of 1,200 cells were counted per slide to determine percent Ki67 positive.

ELISA

The serum from whole blood that was harvested from all the mice were quantified using a E_2–specific enzyme-linked immunosorbent assay (ELISA) (Calbiotech #ES180S-100).

Statistical Analyses

Unless specified, data were analyzed by one-way analysis of variance (ANOVA) followed by Tukey's honestly significant difference (HSD) multiple-range test using GraphPad Prism 8 statistical analysis software or R program (version 3.6.0; R Development Core Team). The difference between control and fulvestrant/RNase H treated groups were evaluated with two-way ANOVA followed by Bonferroni correction. Results are presented as mean ± standard error of the mean (SEM). Data were considered statistically significant at $p<0.05$. Growth curves were fitted to linear regression model, and slopes were compared between control and treatment conditions. Slopes and 95% confidence interval are reported in Table 2.

Results

DNA Damage and TFF1 Gene Expression in Cells Treated with E_2, BP-3, or PP

We monitored γ-H2AX foci as a measure of DNA damage in T47D cells treated with the compounds for 24 h. A dose-dependent increase in γ-H2AX intensity was observed following E_2 treatment (Figure 1A). Treatment with either BP-3 or PP also led to an increase in γ-H2AX intensity. Treatment with BP-3 at 1 or 5 μM increased γ-H2AX intensity in comparison with the control ($p<0.0001$) although we did not observe a dose-dependent increase (1 μM BP-3 vs 5 μM BP-3, Figure 1B). PP treatment also resulted in significantly increased γ-H2AX intensity at 1 and 5 μM in comparison with the control ($p<0.0001$). The γ-H2AX intensity due to PP treatment was dose-dependent, similar to that of E_2 treatment (1 μM PP vs. 5 μM PP, $p<0.0001$) (Figure 1C). We also observed a dose-dependent increase in nuclear γ-H2AX intensity in MCF-7 with treatment of E_2 (10–100 nM), BP-3 (1–30 μM) and PP (1–30 μM) (Figure S1). We confirmed the DNA damage with immunostaining of 53BP1 (P53-binding protein 1), a DNA damage response factor, which localizes to the sites of DNA damage and forms ionization radiation–induced foci. Similar to γ-H2AX intensity, we observed dose-dependent increases in 53BP1 nuclear intensity following treatment with E_2 (10–100 nM) and PP (1–5 μM) incomparison with control in both T47D and MCF-7. BP-3 treatment (1–5 μM) showed increased nuclear 53BP1 intensity over control in both T47D and MCF-7, but only MCF-7 showed dose-dependent increase (Figure 1D and E).

The effect of these compounds on γ-H2AX was contrasted with the mRNA expression of estrogen-responsive gene *TFF1*. Treatment with 10 nM E_2 stimulated a 13.1-fold increase in expression of the estrogen-responsive gene *TFF1*, whereas responses to 5 μM BP-3 or PP did not differ significantly from the control (Figure 2A). The transcriptional responses to E_2 were blocked by treatment with fulvestrant (ICI 182780, 1 μM), demonstrating the dependence on ER. Blocking ER with fulvestrant also significantly reduced the effect of E_2 on γ-H2AX intensity (Figure 2B, $p<0.0001$) and inhibited γ-H2AX intensity in response to 5 μM BP-3 ($p<0.0001$), suggesting that the induction of DNA damage was, in part, dependent on ER. However,

Table 2. Slopes of growth curve showing effect of estradiol (E_2), benzophenone-3 (BP-3), or propylparaben (PP) on T47D cells.

Growth Curve	Slope	95% CI
Control DMSO	0.0107	−0.006811, 0.02821
0.5 nM E_2	0.08495	0.06604, 0.1039
1 μM PP	0.01856	0.003943, 0.03318
10 μM PP	0.06387	0.05225, 0.07550
5 μM BP-3	0.0202	0.008131, 0.03226
50 μM BP-3	0.01581	0.0009721, 0.03064

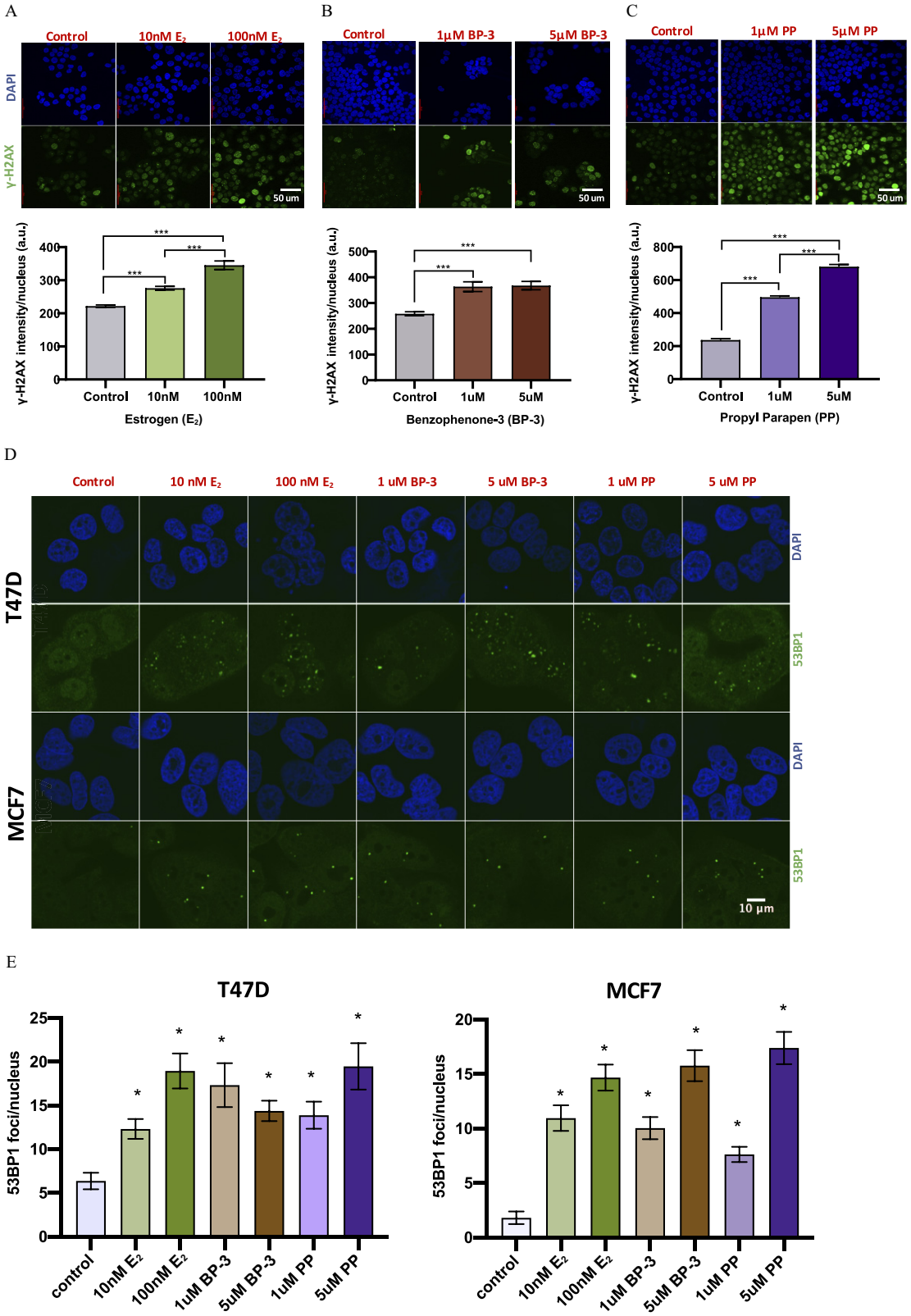

Figure 1. Evaluation of DNA damage in cells treated with 17β-Estradiol (E_2), Benzophenone-3 (BP-3), or Propylparaben (PP) for 24 h. Immunofluorescence (upper panel) and quantification (lower panel) of nuclear γ-H2AX intensity in T47D cells treated with (A) 10 or 100 nM E_2, (B) 1 or 5 μM BP-3, and (C) 1 or 5 μM PP. (D) Immunofluorescence of 53BP1 staining with 10 or 100 nM E_2, 1 or 5 μM BP-3, and 1 or 5 μM PP in T47D (upper panel) and MCF-7 (lower panel). (E) Quantification of nuclear 53BP1 of treatments in (D) in T47D (left panel) and MCF-7 (right panel). $^{***}p < 0.0001$, $^{*}p < 0.01$ compared with control with treatments using one-way analysis of variance (ANOVA) followed by Tukey's honestly significant difference (HSD) multiple-range test. $n = 3$ biological replicates. Scale bar = 50 μM (A–C), 10 μM (D). All graphs show mean ± SEM.

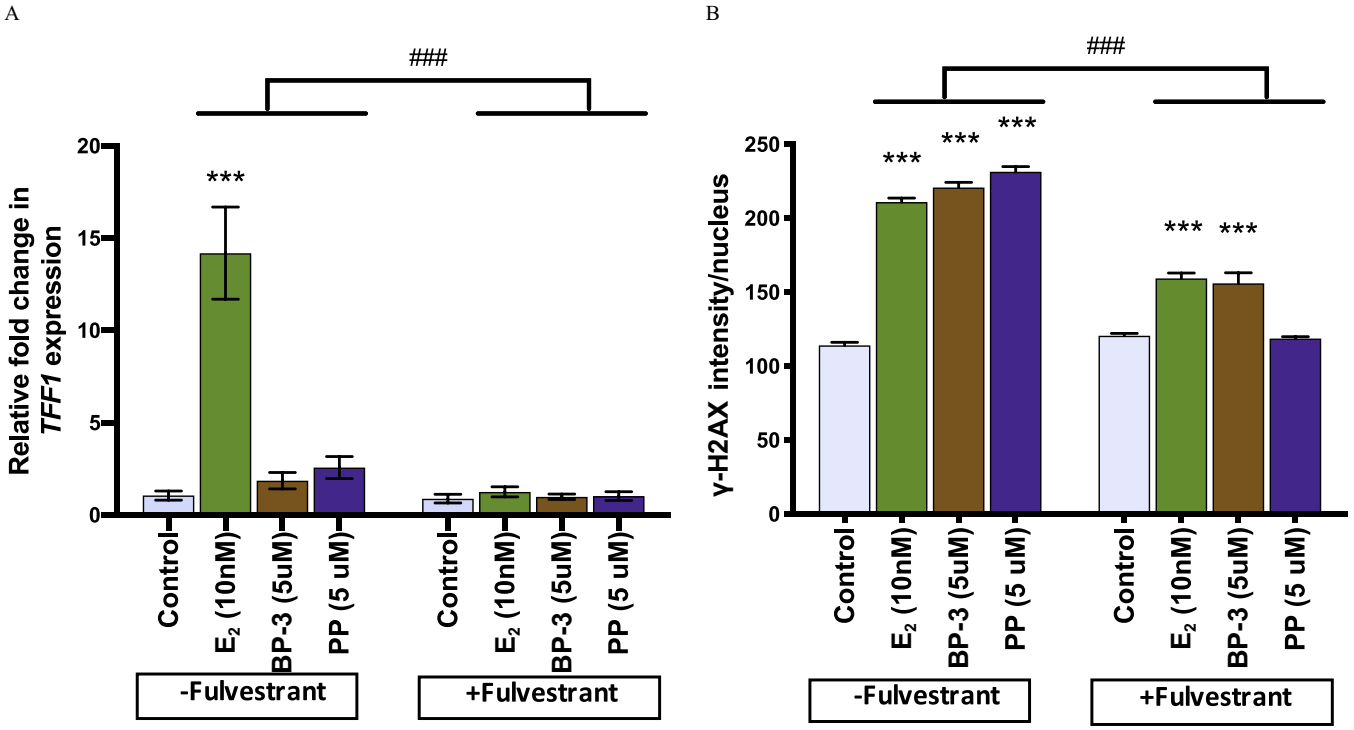

Figure 2. *TFF1* expression and γ-H2AX intensity in T47D cells treated with 17β-estradiol (E_2), benzophenone-3 (BP-3), or propylparaben (PP) for 24 h with or without the ER antagonist fulvestrant. (A) Inhibition of *TFF1* expression following treatment of 10 nM E_2, 5 μM BP-3, and 5 μM PP when cotreated with fulvestrant (ICI 182 780, 1 μM) compared with 10 nM E_2, 5 μM BP-3, and 5 μM PP treatments without fulvestrant. (B) Quantification of nuclear γ-H2AX following cotreatment of fulvestrant (1 μM) with E_2 (10 nM), BP-3 (5 μM), or PP (5 μM) compared with E_2 (10 nM), BP-3 (5 μM), or PP (5 μM) without fulvestrant treatment, respectively. $^{***}p < 0.0001$ compared control to xenoestrogens treatment and $^{###}p < 0.001$ compared with negative fulvestrant and with positive fulvestrant using multiple comparison for 2-way ANOVA. $n = 3$ biological replicates. All graphs show mean ± SEM.

the γ-H2AX foci induced by E_2 and BP-3 was incompletely blocked by fulvestrant in comparison with its inhibition of *TFF1* expression.

Estrogenic Response in Cells Treated with BP-3 and PP

Reporter assays provide a sensitive means to evaluate estrogenic activity on a minimal promoter, whereas endogenous genes containing estrogen-responsive elements provide physiologically relevant targets. To saturate ER responses in these assays, 10 nM E_2 is sufficient; hence, it was used as positive control that is relevant to physiologic E_2 levels (2–70 nM) in women (Table 1). T47D-KBluc cells harbor an integrated ERE-luciferase reporter in which BP-3 showed a lowest-observed-effect at 5 μM with transactivation increasing to a maximum 37% relative transactivation activity (RTA) in comparison with 10 nM E_2 (Figure 3A). In contrast, PP showed 4.7% RTA at 0.5 μM and increased to 288% at 50 μM. To estimate the transactivation activity of the compounds at levels that are relevant to human exposure, we used the published urinary levels of BP-3 and PP (Table 1). At concentrations measured in the 95th percentile of pregnant women, BP-3 had 27.16 ± 6.2%, and PP had 104.07 ± 20.98% RTA (Figure S2, white and black arrows, respectively). Expression of endogenous ER target genes *AREG* and *PGR* were also quantified in T47D and MCF-7 cell lines (Figure 3B and C). Treatment of BP-3 and PP at 1 μM resulted in no significant changes in mRNA expression of *AREG* and *PGR*, a concentration that led to significant increases in DNA damage in both T47D and MCF7 cells (Figure 1). Proliferation induced by these compounds was also compared with control treatment to provide an additional measure of their bioactivity (Figure 3D, Table 2). PP stimulated significant proliferation of T47D cells at 10 μM, but not at 1 μM PP. However, BP-3 had marginal effect at 5 or 50 μM. Low concentrations of BP-3 and PP only marginally increased cell numbers in comparison with control.

R-Loop Formation in T47D Cells Treated with E_2, BP-3, or PP

R-loop formation was investigated as a possible mechanism of DNA damage using the S9.6 antibody to specifically detect DNA:RNA hybrids. Although we observed a basal level of R-loop foci in the vehicle-treated control in T47D cells, nuclear S9.6 foci were significantly increased with 5 μM of BP-3 or PP treatment and comparable with responses with 10 nM E_2. Addition of RNase H to the cells treated with 5 μM BP-3 or PP or 10 nM E_2 abolished the S9.6 intensities, confirming the specificity of S9.6 nuclear staining (Figure 4A and B). Similarly, increase of R-loops formation was obtained with 10 nM E_2, 5 μM BP-3, or 5 μM PP treatment of MCF-7 cells, which was abrogated following RNase H addition post fixation (Figure 4C).

R-Loop Formation in Normal Breast Epithelial Cell Line Treated with E_2, BP-3, or PP

Next, we asked whether R-loops form in normal breast epithelial cells in response to exposures of BP-3 and PP (Figure 5). The 76N-Tert cells do not express endogenous *ESR1*, providing a null background to test ERα-stimulated R-loops. The cells were stably infected with an inducible human *ESR1* (pINDUCER-*ESR1*) (Figure 5A) ERα expression in 76N-Tert-*ESR1* was confirmed with Western blot (Figure 5B). MCF-7 cell lysate was used as a positive control. Immunofluorescence showed 90% of the 76N-Tert-*ESR1* cell population were GFP-positive (ERα expressing) (Figure S3).

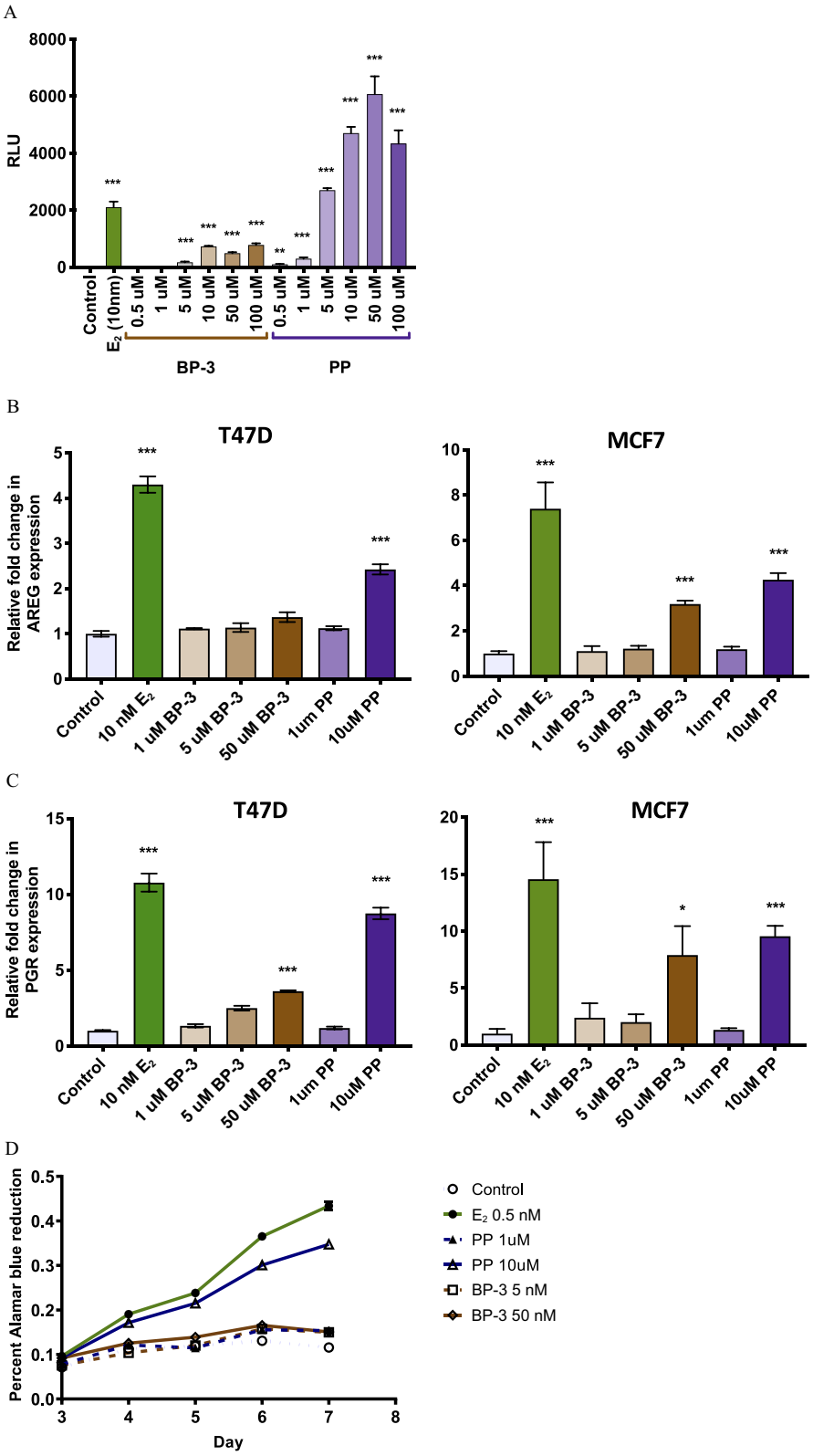

Figure 3. Evaluation of estrogen receptor transactivation and proliferation in cells treated with 17β-estradiol (E_2), benzophenone-3 (BP-3), or propylparaben (PP) for 24 h. (A) Transactivation response (in relative light unit, RLU) of T47D-KBluc cells in response to 10 nM E_2 (green), 0.5–100 μM BP-3 (brown), and 0.5–100 μM PP (violet) treatment. Expression of endogenous genes AREG (B) and PGR (C) with E_2 (10 nM), BP-3 (1 or 5 μM), or PP (1 or 10 μM) treatment as relative fold change over control in T47D (left panel) and MCF-7 (right panel). $^{*}p < 0.05$ and $^{***}p < 0.0001$ compared control with treatments using one-way analysis of variance (ANOVA) followed by Tukey's honestly significant difference (HSD) multiple-range test. $n = 3$ biological replicates. (D) Proliferation of 47D cell as percent of Alamar Blue reduction in response to E_2 (0.5 nM), PP (1 or 10 μM), BP-3 (5 μM), or control. The confidence intervals of the slope are reported in Table 2. All graphs show mean ± SEM.

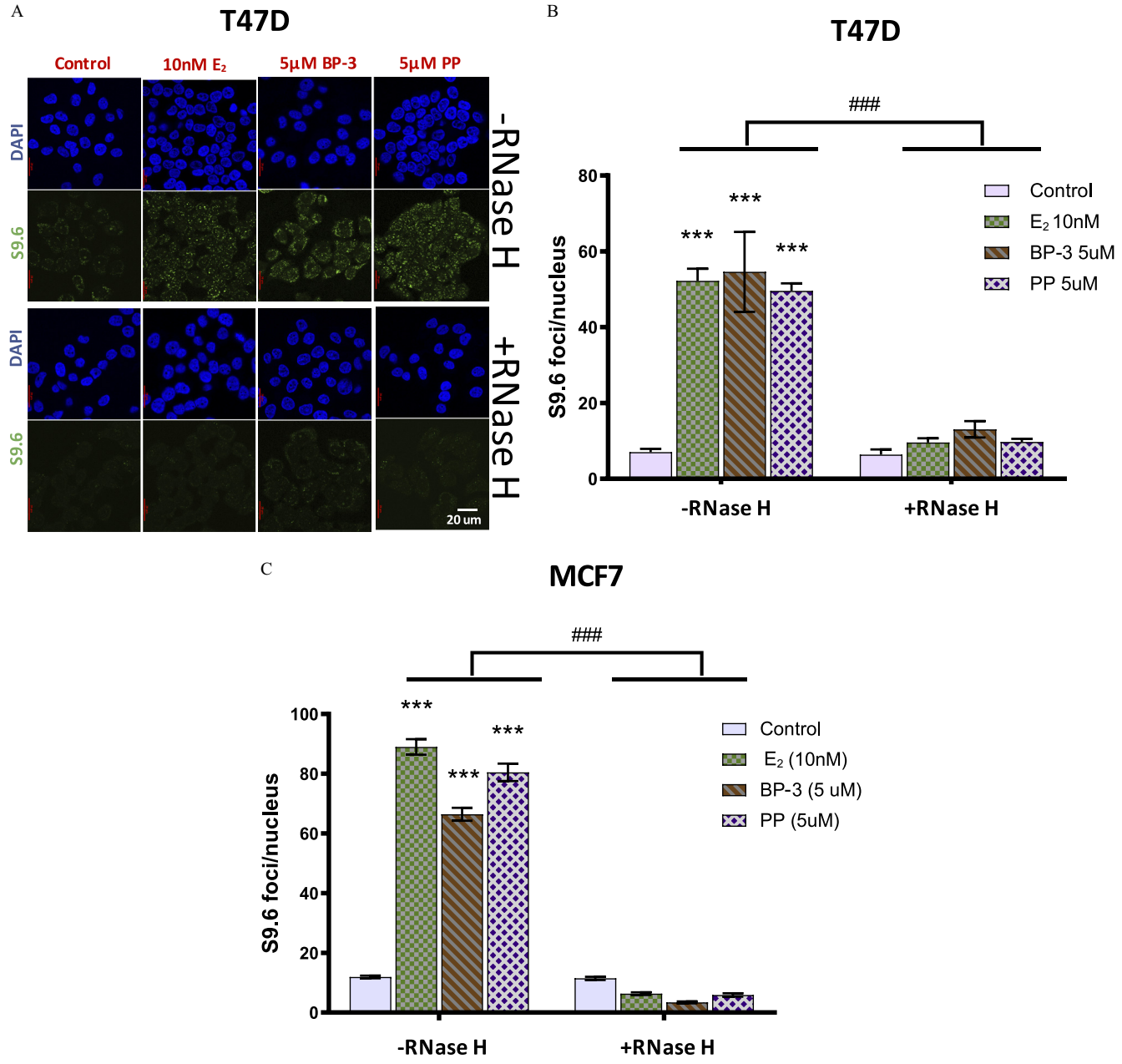

Figure 4. R-loop formation in T47D and MCF7 cells treated with 17β-estradiol (E_2), benzophenone-3 (BP-3), or propylparaben (PP) or vehicle with or without RNase H. (A) Immunostaining of R-loop with S9.6 antibody and DAPI in T47D cells treated with E_2 (10 nM), BP-3 (5 μM) or PP (5 μM) without and with RNase H treatment following fixation. Scale bar = 20 μM. (B) Quantification of the nuclear S9.6 intensity in T47D. (C) Quantification of nuclear S9.6 intensity in MCF-7. $^{***}p < 0.0001$ compared control with xenoestrogens treatment and $^{###}p < 0.001$ compared negative RNase H and with positive RNase H using multiple comparison for 2-way ANOVA. $n = 3$ biological replicates. All graphs show mean ± SEM.

In the parental 76N-Tert cell line, which does not express ERα, treatment with 10 nM E_2, 5 μM BP-3, or 5 μM PP showed low nuclear S9.6 staining. After induction of ERα with doxycycline, 5 μM BP-3 or PP increased the number of nuclear S9.6 foci significantly over vehicle-treated control and was comparable with 10 nM E_2 treatment. RNase H treatment reduced nuclear S9.6 foci in 10 nM E_2 treated as well as 5 μM BP-3 or PP treated 76N-Tert-*ESR1* cell line induced with doxycycline ($p < 0.0001$, Figure 5C and D).

Evaluation of R-Loop Formation and DNA Damage in Mice Treated with E_2, BP-3, or PP

To evaluate the relevance of exposure to xenoestrogens *in vivo*, we treated ovariectomized BALB/c mice orally with E_2 (250 μg/kg/d), BP-3 (3,000 μg/kg/d) or PP (10,000 μg/kg/d) for 4 d (Figure 6A). These doses were used in experiments evaluating effects of chronic exposures on mammary gland development (LaPlante et al. 2018). We observed 3.8-fold higher nuclear S9.6 staining in the mammary epithelium of E_2-treated animals over control-treated animals. Exposure to BP-3 also induced 2.5-fold higher nuclear S9.6 staining in the mammary epithelial cells, whereas PP induced 3.8-fold higher in comparison with control-treated animals (Figure 6B and C). Nuclear γ-H2AX intensity in the mammary gland of E_2- and BP-3-treated animals was significantly higher than animals treated with vehicle control (Figure 6D). Although oral treatment of E_2 stimulated proliferation as shown by higher Ki67 straining and transcriptional activation of ER-target genes (*Areg* and *Pgr*) in the mammary gland, neither

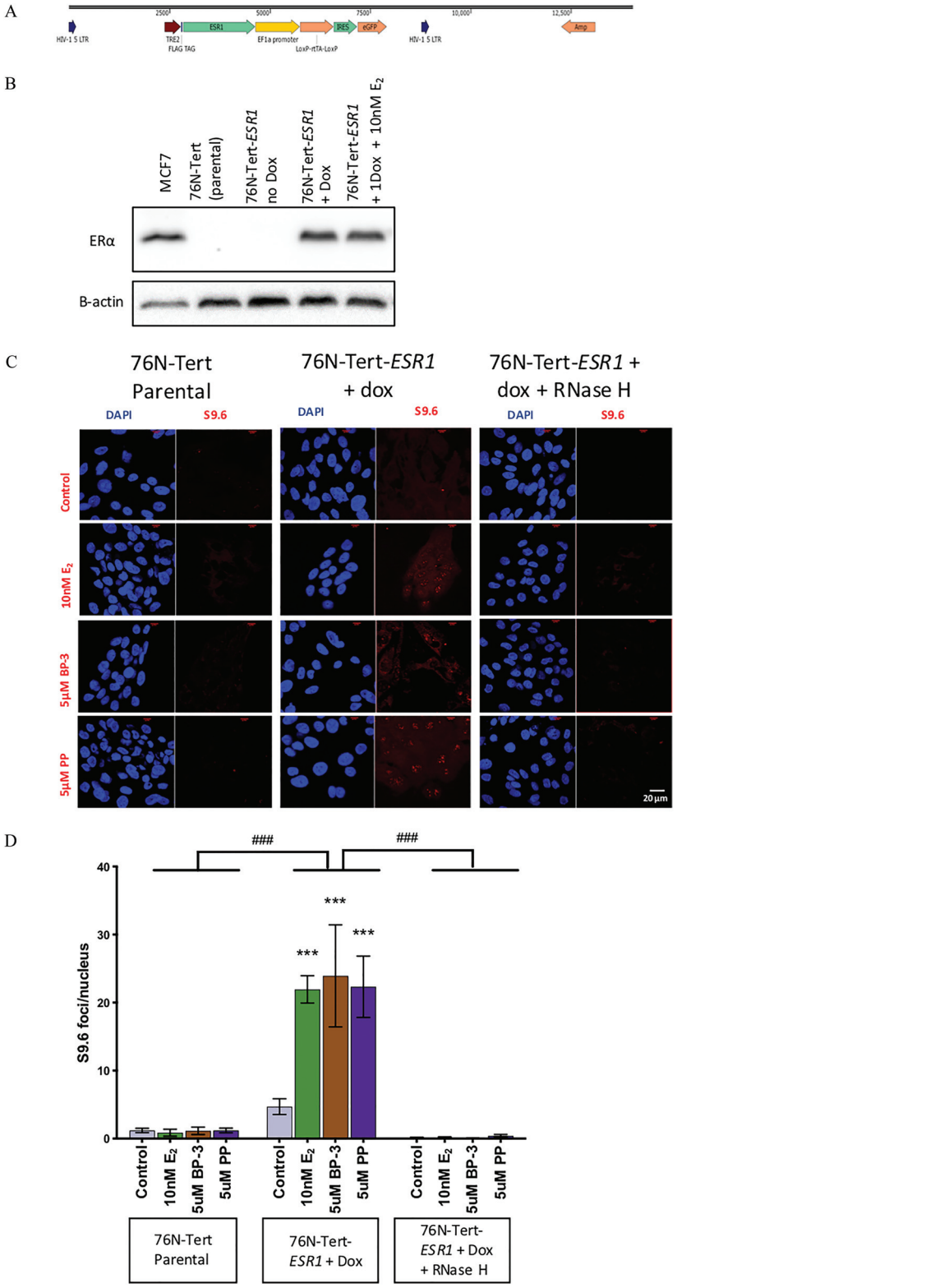

Figure 5. Characterization of 76N-Tert-*ESR1* and R-loop formation in 76N-Tert-*ESR1* following treatment with 17β-estradiol (E_2), benzophenone-3 (BP-3) or propylparaben (PP) with and without RNase H. (A) Map of pIN-ESR1 construct *ESR1* insertion next to doxycycline(dox) inducible TRE_2 promoter. (B) Western blot ERα (upper panel) with MCF-7 as positive control (lane 1), 76N-Tert parental (lane 2), 76N-Tert-*ESR1* without dox (lane 3), 76N-Tert-*ESR1* with dox (lane 4), and 76N-Tert-*ESR1* with dox and E_2 (10 nM) treatment and β-actin as loading control (lower panel). (C) Immunostaining with S9.6 antibody and DAPI with 10 nM E_2, 5 μM BP-3, or 5 μM PP treatment to parental 76N-Tert cells (upper panel), to 76N-Tert-ESR1 with dox induction (middle panel) without or with RNase H treatment (lower panel). Scale bar = 20 μM. (D) Quantification of nuclear S9.6 intensity in (C). $^{***}p < 0.0001$ compared control with xenoestrogens treatment and $^{###}p < 0.001$ compared among 76N-Tert Parental, 76N-Tert with dox and E_2 (10 nM) negative RNase H and 76N-Tert with dox and E_2 (10 nM) positive RNase H using multiple comparison for 2-way ANOVA. $n = 3$ biological replicates. All graphs show mean ± SEM.

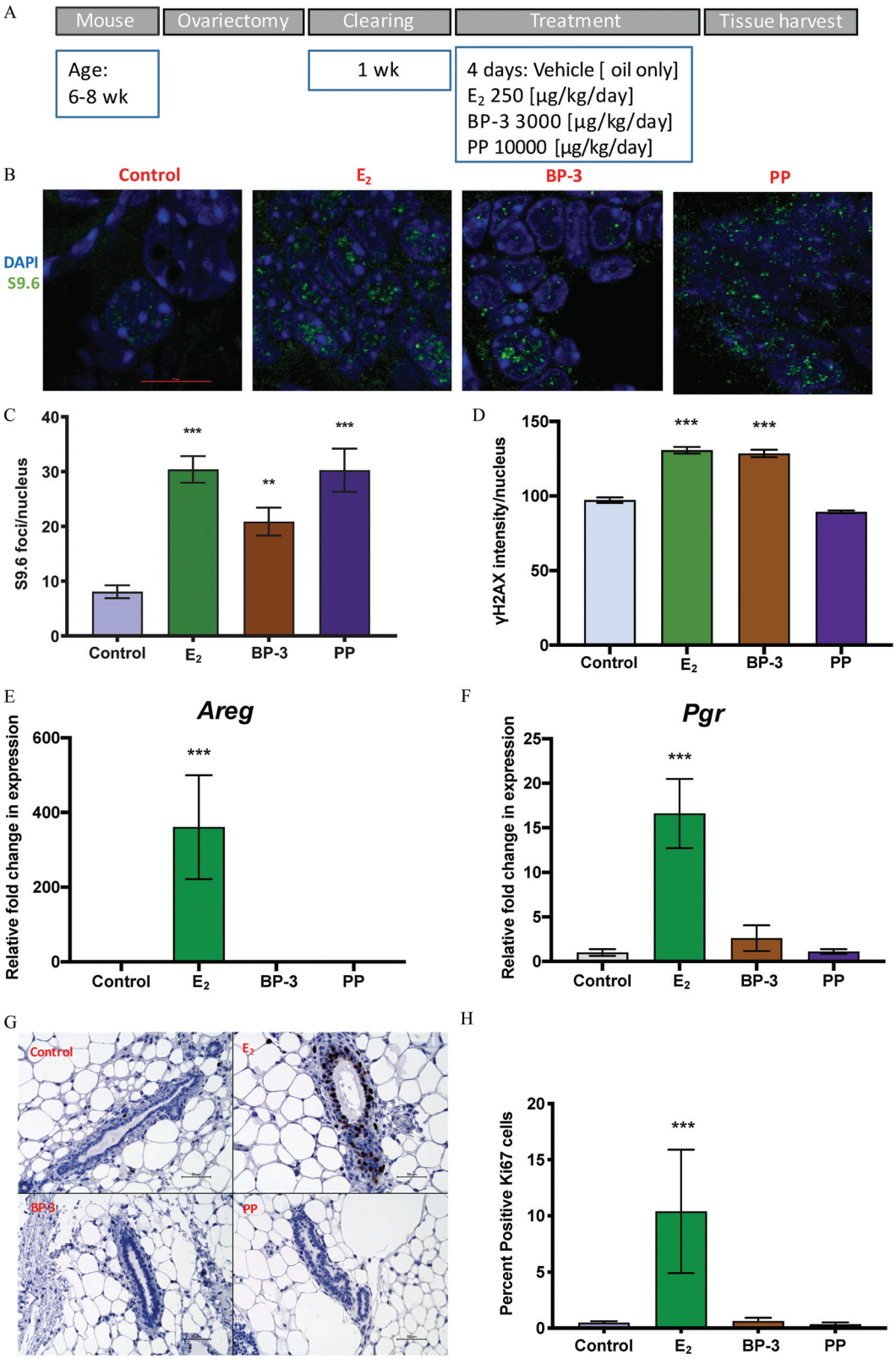

Figure 6. Acute exposure of xenoestrogens in mice. (A) Schematic of experimental design and exposure period. (B) Immunostaining of mouse mammary epithelium with S9.6 antibody harvested from mice treated with E_2, BP-3, or PP. Each image shows a ductal structure with luminal and myo-epithelial cell nucleus (blue) and R-loop (green) inside the nucleus. Scale bar = 10 µM. Quantification of the immunostaining data for S9.6 (C) and γ-H2AX (D). Expression of *Areg* (E) and *Pgr* (F) from mouse mammary gland. $n = 3$ biological replicates. Ki67 straining of luminal epithelial cells (G) and percent of Ki67 strained cells per luminal cells counted (H). Scale bar = 50 µM [Number of biological replicates (n): control (5), E_2 (8), BP-3 (12), PP (10)] $^{***}p < 0.0001$, $^{**}p < 0.01$ compared control with treatments using one-way analysis of variance (ANOVA) followed by Tukey's honestly significant difference (HSD) multiple-range test. All graphs show mean ± SEM.

BP-3 nor PP elicited significant responses (Figure 6 E–H). Similarly, elevated serum levels of E_2 and uterine weight was observed only in E_2-treated mice (Figure S4).

Discussion

Exposure of xenoestrogens was implicated in breast cancer risk (Pastor-Barriuso et al. 2016) as well as resistance to breast cancer treatment (Goodson et al. 2011; Warth et al. 2018) due to their endocrine actions. The median urinary level of BP-3 was 0.137 μM, and PP was 0.161 μM in nonpregnant women in participating in the NHANES by the CDC (Calafat et al. 2010; Woodruff et al. 2011). The serum levels of BP-3 was reported to be approximately 0.87 μM (200 μg/L) following exposure in women (Janjua et al. 2004; Matta et al. 2019; Tarazona et al. 2013). In addition, the urinary concentrations of xenoestrogens observed in pregnant women were higher than in the general population, with median urinary concentrations of BP-3 and PP being 0.47 μM and 0.253 μM, respectively, and the 95th percentile concentrations in pregnant women being 29.5 μM BP-3 and 3.26 μM PP (Table 1). This finding raises the possibility that women may have higher exposure during pregnancy due to use of creams and lotions or that absorption and metabolism may be altered in pregnancy. These compounds were also found in normal tissues of women undergoing mastectomy for primary breast cancer (Barr et al. 2012; Barr et al. 2018) and in milk collected during the period of sunscreen use from three different cohorts of mothers of singleton children (Schlumpf et al. 2010). However, based on measures of transcriptional activity in MCF7 human breast cancer cell lines (Byford et al. 2002; Kerdivel et al. 2013), typical exposures to BP-3 and PP would appear to pose a minimal risk for breast cancer through ER-mediated transcriptional activation of target genes.

Estrogens and their metabolites have been shown to induce direct DNA damage. However, DNA damage by catechol estrogens from ER-negative cell lines requires concentrations that are 100-fold greater than the average circulating concentrations in women (Cavalieri and Rogan 2016; Savage et al. 2014; Xu et al. 2007). BP-3 and PP were shown to have the potential to cause DNA damage independent of ER transactivation, based on experiments on ER-negative cell lines. For example, treatment of BP-3 (10 μM) induced γ-H2AX foci in normal human keratin cell lines (Kim et al. 2018) and PP (50 μM) showed 8-Hydroxy-2-deoxyguanosine (8-OHdG) release in Vero cells (derived from monkey kidney) (Pérez Martín et al. 2010). However, these levels exceeded typical concentrations measured in human populations (Table 1).

In the breast, epithelial cells with functional ERα, we observed DNA damage at physiologic concentrations of E_2. BP-3 and PP also caused DNA damage at low concentrations (1–5 μM) (Figure 1). Both the nuclear γ-H2AX and 53BP1 foci were diminished by fulvestrant, suggesting ERα dependency of DNA damage. At these low concentrations (1 μM of PP and 1–5 μM of BP-3), we did not observe ER-mediated transcriptional response in target genes. Instead, we observed R-loop formation. We also observed increases in R-loops and γ-H2AX in the mammary epithelial cells of ovariectomized BALB/c mice orally treated with BP-3 or PP at doses designed to model environmental exposures in humans (Figure 6D). The doses of BP-3 and PP used in mice were not sufficient to affect transcription of *Areg* or *Pgr* (Figure 6E–F) or proliferation of mammary epithelium (Figure 6G–H) in comparison with control treatments, nor were they sufficient to alter uterine weights in comparison with the control treatment in ovariectomized mice (Figure S4). This finding for BP-3 was supported by a previous study (LaPlante et al. 2018). These results with BP-3 and PP are consistent with the idea that in mammary epithelial cells of human and mice, the formation of R-loops and DNA damage is ER-dependent but is separable from gene transcription and proliferative responses.

ER-mediated DNA double-strand breaks was shown to form by collision of R-loop formed during active transcription (cotranscriptional R-loop) and replication fork in MCF7 cells (Stork et al. 2016). Alternatively, R-loop formation can occur with RNA Polymerase II pausing, which results in no increase of gene expression but leads to DNA damage (Hatchi et al. 2015; Shivji et al. 2018; Zhang et al. 2017). Indeed, our results showed that, BP-3 and PP induced formation of R-loops and DNA damage (Figure 7) but did not lead to detectable increases in full-length transcripts of *TFF1*, *AREG*, or *PGR*.

Experiments performed using a normal breast epithelial cell line 76N-Tert expressing inducible ERα treated with E_2, BP-3, and PP provided *a*) additional evidence that the R-loop formation and DNA damage were ERα-dependent and *b*) that normal breast epithelial cells were susceptible to DNA damage by xenoestrogens. This finding raises the possibility that a subset of women bearing variants of R-loop processing factors may be particularly susceptible to the genotoxic effects of xenoestrogens such as BP-3 and PP. More than 300 R-loop binding proteins have been identified (Wang et al. 2018). A number of such factors were recently shown to be involved in the resolution of R-loops to limit DNA damage, including TopI (Tuduri et al. 2009), BRCA1 (Hatchi et al. 2015), BRCA2 (Shivji et al. 2018), SETX (Cohen et al. 2018; Hatchi et al. 2015), Aquaris (Sollier et al. 2014), THO/THREX complex (Bhatia et al. 2014; Gómez-González et al. 2011), BuGZ, and Bub (Wan et al. 2015). For example, recruitment of BRCA1/SETX was important for R-loop mediated transcriptional termination. As a consequence, the mutational rate of termination regions where BRCA/SETX colocalize was higher in BRCA1-deficient tumors in comparison with BRCA1-WT tumors (Hatchi et al. 2015). Premalignant breast lesions such as atypical hyperplasia expressed higher levels of ERα (Gregory et al. 2019) and thus may be especially sensitive to the genotoxic effects of these xenoestrogens. Therefore, limiting exposure to personal care products and foods containing these chemicals may be valuable for this subset of women.

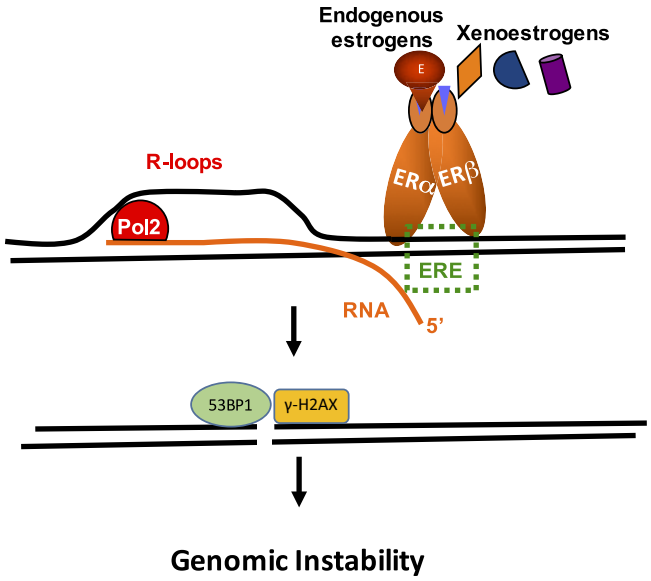

Figure 7. A schematic model for ER-dependent DNA damage. E_2 or xenoestrogens binding to the ER recruit ER to the estrogen response element (ERE) in the promoter and forms R-loop. Persistence of R-loop in the promoter introduces DNA damage.

However, the present studies do not show a direct risk of exposure to these compounds on subsequent breast cancer. Although chronic exposure to low levels of DNA damage have the potential to induce mutations that either initiate or promote carcinogenesis, the experiments were not designed to demonstrate a causal effect of BP-3 or PP on mammary tumors or breast carcinogenesis. The DNA damage observed was associated with the formation of ERα-dependent R-loops, but it is unclear whether ERβ also contributes to the formation of R-loops or may mitigate this. Although many tissues express ERs, they vary in the levels of ERα and ERβ as well as expression of DNA repair factors and proficiency of resolving R-loops. Therefore, this mechanism of DNA damage may be limited to the breast epithelium of a subset of individuals. Also unclear is how combinations of environmental xenoestrogens may interact to augment or dissipate the genotoxicity through competing actions on ER. Nonetheless, the data presented here reveal a need to consider the unique potential for genotoxicity of environmental xenoestrogens in tissues expressing ERs.

These studies demonstrated that xenoestrogens possessed the potential for genotoxic activity that was mediated by ERα through the formation of R-loops and DNA double-strand breaks. These genotoxic effects were observed at concentrations well below those necessary for detectable transcriptional activation. Therefore, R-loop forming capacity provides a valuable end point to consider when evaluating the safety and activity of environmental chemicals. The inducible expression of ERα in normal breast cells provides a tool with which to quantify the variation in sensitivity to these compounds among individuals and to determine whether a subset of individuals is preferentially susceptible to the genotoxic activities.

Acknowledgments

Research reported in this publication was supported, in part, by the National Institute of Environmental Health Sciences of the National Institutes of Health under award number U01ES026140 (D.J.J., S.S.S.), the Department of Defense under contract #W81XWH-15-1-0217 (D.J.J.), the Rays of Hope Center for Breast Cancer Research (D.J.J.), and University Grants Commission (India) for Raman Fellowship for postdoctoral research (P.D.M.). Protocol for S9.6 immunofluorescence in cells was kindly provided by G. Capranico, Professor of Molecular Biology, University of Bologna, Italy. The microscopy data was gathered in the Light Microscopy Facility and Nikon Center of Excellence at the Institute for Applied Life Sciences, UMass Amherst, with support from the Massachusetts Life Sciences Center and help from J. Chambers. The authors thank J. Kane and the Applied Molecular Biotechnology Program for assistance in preparing expression vectors. The authors also thank A. Symington for valuable discussions throughout the project.

References

Alamer M, Darbre PD. 2018. Effects of exposure to six chemical ultraviolet filters commonly used in personal care products on motility of MCF-7 and MDA-MB-231 human breast cancer cells in vitro. J Appl Toxicol 38(2):148–159-159, PMID: 28990245, https://doi.org/10.1002/jat.3525.

Andersson S, Davis D, Dahlbäck H, Jörnvall H, Russell DW. 1989. Cloning, structure, and expression of the mitochondrial cytochrome P-450 sterol 26-hydroxylase, a bile acid biosynthetic enzyme. J Biol Chem 264(14):8222–8229, PMID: 2722778.

Barr L, Alamer M, Darbre PD. 2018. Measurement of concentrations of four chemical ultraviolet filters in human breast tissue at serial locations across the breast. J Appl Toxicol 38(8):1112–1120, PMID: 29658634, https://doi.org/10.1002/jat.3621.

Barr L, Metaxas G, Harbach CA, Savoy LA, Darbre PD. 2012. Measurement of paraben concentrations in human breast tissue at serial locations across the breast from axilla to sternum. J Appl Toxicol 32(3):219–232, PMID: 22237600, https://doi.org/10.1002/jat.1786.

Bhatia V, Barroso SI, García-Rubio ML, Tumini E, Herrera-Moyano E, Aguilera A. 2014. BRCA2 prevents R-loop accumulation and associates with TREX-2 mRNA export factor PCID2. Nature 511(7509):362–365, PMID: 24896180, https://doi.org/10.1038/nature13374.

Buteau-Lozano H, Ancelin M, Lardeux B, Milanini J, Perrot-Applanat M. 2002. Transcriptional regulation of vascular endothelial growth factor by estradiol and tamoxifen in breast cancer cells. Cancer Res 62(17):4977–4984, PMID: 12208749.

Byford JR, Shaw LE, Drew MG, Pope GS, Sauer MJ, Darbre PD. 2002. Oestrogenic activity of parabens in MCF7 human breast cancer cells. J Steroid Biochem Mol Biol 80(1):49–60, PMID: 11867263, https://doi.org/10.1016/S0960-0760(01)00174-1.

Calafat AM, Wong LY, Ye X, Reidy JA, Needham LL. 2008. Concentrations of the sunscreen agent benzophenone-3 in residents of the United States: National Health and Nutrition Examination Survey 2003–2004. Environ Health Perspect 116(7):893–897, PMID: 18629311, https://doi.org/10.1289/ehp.11269.

Calafat AM, Ye X, Wong LY, Bishop AM, Needham LL. 2010. Urinary concentrations of four parabens in the U.S. population: NHANES 2005–2006. Environ Health Perspect 118(5):679–685, PMID: 20056562, https://doi.org/10.1289/ehp.0901560.

Cavalieri EL, Rogan EG. 2016. Depurinating estrogen-DNA adducts, generators of cancer initiation: their minimization leads to cancer prevention. Clin Transl Med 5(1):12, PMID: 26979321, https://doi.org/10.1186/s40169-016-0088-3.

Chao Q, Jeffrey C, Yiwei Z, Anjana VY, Sambasiva MR, Yi-Jun JZ. 2002. Identification of protein arginine methyltransferase 2 as a coactivator for estrogen receptor alpha. J Biol Chem 277(32):28624–30, PMID: 12039952, https://doi.org/10.1074/jbc.M201053200.

Clarke RB, Howell A, Anderson E. 1997. Estrogen sensitivity of normal human breast tissue in vivo and implanted into athymic nude mice: analysis of the relationship between estrogen-induced proliferation and progesterone receptor expression. Breast Cancer Res Treat 45(2):121–133, PMID: 9342437, https://doi.org/10.1023/a:1005805831460.

Cohen S, Puget N, Lin YL, Clouaire T, Aguirrebengoa M, Rocher V. 2018. Senataxin resolves RNA:DNA hybrids forming at DNA double-strand breaks to prevent translocations. Nat Commun 9(1):533, PMID: 29416069, https://doi.org/10.1038/s41467-018-02894-w.

Cummings SR, Eckert S, Krueger KA, Grady D, Powles TJ, Cauley JA. 1999. The effect of raloxifene on risk of breast cancer in postmenopausal women: results from the MORE randomized trial. Multiple Outcomes of Raloxifene Evaluation. JAMA 281:2189–2197, PMID: 10376571, https://doi.org/10.1001/jama.281.23.2189.

Cuzick J, International Breast Cancer Intervention Study. 2001. A brief review of the International Breast Cancer Intervention Study (IBIS), the other current breast cancer prevention trials, and proposals for future trials. Ann NY Acad Sci 949:123–133, PMID: 11795344, https://doi.org/10.1111/j.1749-6632.2001.tb04010.x.

Dallal CM, Tice JA, Buist DS, Bauer DC, Lacey JV Jr, Cauley JA, et al. 2014. Estrogen metabolism and breast cancer risk among postmenopausal women: a case-cohort study within B∼FIT. Carcinogenesis 35(2):346–355, PMID: 24213602, https://doi.org/10.1093/carcin/bgt367.

EBCTCG (Early Breast Cancer Trialists' Collaborative Group). 2015. Aromatase inhibitors versus tamoxifen in early breast cancer: patient-level meta-analysis of the randomised trials. Lancet 386:1341–1352, PMID: 26211827, https://doi.org/10.1016/S0140-6736(15)61074-1.

EC (European Commission). 2014. Commission Regulation (EU) No. 1004/2014 of 18 September 2014 amending Annex V to Regulation (EC) No. 1223/2009 of the European Parliament and of the Council on cosmetic products Text with EEA relevance. https://op.europa.eu/en/publication-detail/-/publication/a22d3948-4545-11e4-a0cb-01aa75ed71a1/language-en [accessed 5 February 2019].

EC. 2017. Commission Regulation (EU) 2017/238 of 10 February 2017 amending Annex VI to Regulation (EC) No. 1223/2009 of the European Parliament and of the Council on cosmetic products. http://data.europa.eu/eli/reg/2017/238/oj [accessed 5 February 2019].

Feinleib M. 1968. Breast cancer and artificial menopause: a cohort study. J Natl Cancer Inst 41(2):315–329, PMID: 5671283.

Fuhrman BJ, Schairer C, Gail MH, Boyd-Morin J, Xu X, Sue LY, et al. 2012. Estrogen metabolism and risk of breast cancer in postmenopausal women. J Natl Cancer Inst 104(4):326–339, PMID: 22232133, https://doi.org/10.1093/jnci/djr531.

Fullwood MJ, Liu MH, Pan YF, Liu J, Xu H, Mohamed YB, et al. 2009. An oestrogen-receptor-alpha-bound human chromatin interactome. Nature 462(7269):58–64-64, PMID: 19890323, https://doi.org/10.1038/nature08497.

Fussell KC, Udasin RG, Smith PJ, Gallo MA, Laskin JD. 2011. Catechol metabolites of endogenous estrogens induce redox cycling and generate reactive oxygen species in breast epithelial cells. Carcinogenesis 32(8):1285–1293, PMID: 21665890, https://doi.org/10.1093/carcin/bgr109.

Gómez-González B, García-Rubio M, Bermejo R, Gaillard H, Shirahige K, Marín A, et al. 2011. Genome-wide function of THO/TREX in active genes prevents R-

loop-dependent replication obstacles. EMBO J 30(15):3106–3119-3119, PMID: 21701562, https://doi.org/10.1038/emboj.2011.206.
Gonzalez H, Farbrot A, Larkö O, Wennberg AM. 2006. Percutaneous absorption of the sunscreen benzophenone-3 after repeated whole-body applications, with and without ultraviolet irradiation. Br J Dermatol 154(2):337–340, PMID: 16433806, https://doi.org/10.1111/j.1365-2133.2005.07007.x.
Goodson WH 3rd, Luciani MG, Sayeed SA, Jaffee IM, Moore DH 2nd, Dairkee SH. 2011. Activation of the mTOR pathway by low levels of xenoestrogens in breast epithelial cells from high-risk women. Carcinogenesis 32(11):1724–1733, PMID: 21890461, https://doi.org/10.1093/carcin/bgr196.
Goss PE, Ingle JN, Alés-Martínez JE, Cheung AM, Chlebowski RT, Wactawski-Wende J, et al. 2011. Exemestane for breast-cancer prevention in postmenopausal women. N Engl J Med 364(25):2381–2391, PMID: 21639806, https://doi.org/10.1056/NEJMoa1103507.
Gregory KJ, Roberts AL, Conlon EM, Mayfield JA, Hagen MJ, Crisi GM, et al. 2019. Gene expression signature of atypical breast hyperplasia and regulation by SFRP1. Breast Cancer Res 21(1):76, PMID: 31248446, https://doi.org/10.1186/s13058-019-1157-5.
Hatchi E, Skourti-Stathaki K, Ventz S, Pinello L, Yen A, Kamieniarz-Gdula K, et al. 2015. BRCA1 recruitment to transcriptional pause sites is required for R-loop-driven dna damage repair. Mol Cell 57(4):636–647-647, PMID: 25699710, https://doi.org/10.1016/j.molcel.2015.01.011.
Henderson BE, Feigelson HS. 2000. Hormonal carcinogenesis. Carcinogenesis 21(3):427–433, PMID: 10688862, https://doi.org/10.1093/carcin/21.3.427.
Henderson BE, Ross R, Bernstein L. 1988. Estrogens as a cause of human cancer: the Richard and Hinda Rosenthal Foundation award lecture. Cancer Res 48(2):246–253, PMID: 2825969.
Huang Y, Fernandez SV, Goodwin S, Russo PA, Russo IH, Sutter TR, et al. 2007. Epithelial to mesenchymal transition in human breast epithelial cells transformed by 17beta-estradiol. Cancer Res 67(23):11147–11157, PMID: 18056439, https://doi.org/10.1158/0008-5472.CAN-07-1371.
Janjua NR, Mogensen B, Andersson A-M, Petersen JHH, Henriksen M, Skakkebaek NE, et al. 2004. Systemic absorption of the sunscreens benzophenone-3, octyl-methoxycinnamate, and 3-(4-methyl-benzylidene) camphor after whole-body topical application and reproductive hormone levels in humans. J Invest Dermatol 123(1):57–61, PMID: 15191542, https://doi.org/10.1111/j.0022-202X.2004.22725.x.
Kerdivel G, Guevel R, Habauzit D, Brion F, Ait-Aissa S, Pakdel F. 2013. Estrogenic potency of benzophenone UV filters in breast cancer cells: proliferative and transcriptional activity substantiated by docking analysis. PLoS One 8(4):e60567, PMID: 23593250, https://doi.org/10.1371/journal.pone.0060567.
Khanna S, Dash PR, Darbre PD. 2014. Exposure to parabens at the concentration of maximal proliferative response increases migratory and invasive activity of human breast cancer cells in vitro. J Appl Toxicol 34(9):1051–1059, PMID: 24652746, https://doi.org/10.1002/jat.3003.
Kim HJ, Lee E, Lee M, Ahn S, Kim J, Liu J, et al. 2018. Phosphodiesterase 4B plays a role in benzophenone-3-induced phototoxicity in normal human keratinocytes. Toxicol Appl Pharmacol 338:174–181-181, PMID: 29183759, https://doi.org/10.1016/j.taap.2017.11.021.
Kunisue T, Chen Z, Louis GM, Sundaram R, Hediger ML, Sun L, et al. 2012. Urinary concentrations of benzophenone-type UV filters in U.S. women and their association with endometriosis. Environ Sci Technol 46(8):4624–4632, PMID: 22417702, https://doi.org/10.1021/es204415a.
LaPlante CD, Bansal R, Dunphy KA, Jerry DJ, Vandenberg LN. 2018. Oxybenzone alters mammary gland morphology in mice exposed during pregnancy and lactation. J Endocr Soc 2(8):903–921, PMID: 30057971, https://doi.org/10.1210/js.2018-00024.
Liao C, Kannan K. 2014. Widespread occurrence of benzophenone-type UV light filters in personal care products from China and the United States: an assessment of human exposure. Environ Sci Technol 48(7):4103–4109, PMID: 24588714, https://doi.org/10.1021/es405450n.
Liehr JG, Sirbasku DA, Jurka E, Randerath K, Randerath E. 1988. Inhibition of estrogen-induced renal carcinogenesis in male Syrian hamsters by tamoxifen without decrease in DNA adduct levels. Cancer Res 48(4):779–783, PMID: 3338075.
Majewski AR, Chuong LM, Neill HM, Roberts AL, Jerry DJ, Dunphy KA. 2018. Sterilization of silastic capsules containing 17β-estradiol for effective hormone delivery in Mus musculus. J Am Assoc Lab Anim Sci 57(6):679–685, PMID: 30314533, https://doi.org/10.30802/AALAS-JAALAS-18-000030.
Martino S, Cauley JA, Barrett-Connor E, Powles TJ, Mershon J, Disch D, et al. 2004. Continuing outcomes relevant to Evista: breast cancer incidence in postmenopausal osteoporotic women in a randomized trial of raloxifene. J Natl Cancer Inst 96(23):1751–1761, PMID: 15572757, https://doi.org/10.1093/jnci/djh319.
Matta MK, Zusterzeel R, Pilli NR, Patel V, Volpe DA, Florian J, et al. 2019. Effect of sunscreen application under maximal use conditions on plasma concentration of sunscreen active ingredients: a randomized clinical trial. JAMA 321(21):2082–2091, PMID: 31058986, https://doi.org/10.1001/jama.2019.5586.
Meerbrey KL, Hu G, Kessler JD, Roarty K, Li MZ, Fang JE, et al. 2011. The pINDUCER lentiviral toolkit for inducible RNA interference in vitro and in vivo. Proc Natl Acad Sci USA 108(9):3665–3670, PMID: 21307310, https://doi.org/10.1073/pnas.1019736108.
Mobley JA, Brueggemeier RW. 2004. Estrogen receptor-mediated regulation of oxidative stress and DNA damage in breast cancer. Carcinogenesis 25(1):3–9, PMID: 14514655, https://doi.org/10.1093/carcin/bgg175.
Molins-Delgado D, Olmo-Campos MDM, Valeta-Juan G, Pleguezuelos-Hernández V, Barceló D, Díaz-Cruz MS. 2018. Determination of UV filters in human breast milk using turbulent flow chromatography and babies' daily intake estimation. Environ Res 161:532–539, PMID: 29232646, https://doi.org/10.1016/j.envres.2017.11.033.
Moore SC, Matthews CE, Ou Shu X, Yu K, Gail MH, Xu X. 2016. Endogenous estrogens, estrogen metabolites, and breast cancer risk in postmenopausal Chinese women. J Natl Cancer Inst 108(10), PMID: 27193440, https://doi.org/10.1093/jnci/djw103.
Musgrove EA, Sutherland RL. 1994. Cell cycle control by steroid hormones. Semin Cancer Biol 5(5):381–389, PMID: 7849266.
Okereke CS, Abdel-Rhaman MS, Friedman MA. 1994. Disposition of benzophenone-3 after dermal administration in male rats. Toxicol Lett 73(2):113–122, PMID: 8048080, https://doi.org/10.1016/0378-4274(94)90101-5.
O'Leary P, Boyne P, Flett P, Beilby J, James I. 1991. Longitudinal assessment of changes in reproductive hormones during normal pregnancy. Clin Chem 37(5):667–672, PMID: 1827758.
Pastor-Barriuso R, Fernández MF, Castaño-Vinyals G, Whelan D, Pérez-Gómez B, Llorca J, et al. 2016. Total effective xenoestrogen burden in serum samples and risk for breast cancer in a population-based multicase-control study in Spain. Environ Health Perspect 124(10):1575–1582, PMID: 27203080, https://doi.org/10.1289/EHP157.
Pérez Martín J, Peropadre A, Herrero Ó, Freire P, Labrador V, Hazen M. 2010. Oxidative DNA damage contributes to the toxic activity of propylparaben in mammalian cells. Mutat Res/Genetic Toxicol Environ Mutagenesis 702(1):86–91, PMID: 20682357, https://doi.org/10.1016/j.mrgentox.2010.07.012.
Periyasamy M, Patel H, Lai CF, Nguyen V, Nevedomskaya E, Harrod A, et al. 2015. APOBEC3B-mediated cytidine deamination is required for estrogen receptor action in breast cancer. Cell Rep 13(1):108–121, PMID: 26411678, https://doi.org/10.1016/j.celrep.2015.08.066.
Philippat C, Wolff MS, Calafat AM, Ye X, Bausell R, Meadows M, et al. 2013. Prenatal exposure to environmental phenols: concentrations in amniotic fluid and variability in urinary concentrations during pregnancy. Environ Health Perspect 121(10):1225–1231, PMID: 23942273, https://doi.org/10.1289/ehp.1206335.
Preston-Martin S, Pike MC, Ross RK, Jones PA, Henderson BE. 1990. Increased cell division as a cause of human cancer. Cancer Res 50(23):7415–7421, PMID: 2174724.
Rajapakse N, Butterworth M, Kortenkamp A. 2005. Detection of DNA strand breaks and oxidized DNA bases at the single-cell level resulting from exposure to estradiol and hydroxylated metabolites. Environ Mol Mutagen 45(4):397–404, PMID: 15662657, https://doi.org/10.1002/em.20104.
Roy D, Liehr JG. 1999. Estrogen, DNA damage and mutations. Mutat Res/Fundamental and Mol Mech Mutagenesis 424(1–2):107–115, PMID: 10064854, https://doi.org/10.1016/S0027-5107(99)00012-3.
Russo J, Hasan Lareef M, Balogh G, Guo S, Russo IH. 2003. Estrogen and its metabolites are carcinogenic agents in human breast epithelial cells. J Steroid Biochem Mol Biol 87(1):1–25, PMID: 14630087, https://doi.org/10.1016/s0960-0760(03)00390-x.
Sampson JN, Falk RT, Schairer C, Moore SC, Fuhrman BJ, Dallal CM, et al. 2017. Association of estrogen metabolism with breast cancer risk in different cohorts of postmenopausal women. Cancer Res 77(4):918–925, PMID: 28011624, https://doi.org/10.1158/0008-5472.CAN-16-1717.
Santen R, Cavalieri E, Rogan E, Russo J, Guttenplan J, Ingle J, et al. 2009. Estrogen mediation of breast tumor formation involves estrogen receptor-dependent, as well as independent, genotoxic effects. Ann NY Acad Sci 1155:132–140, PMID: 19250200, https://doi.org/10.1111/j.1749-6632.2008.03685.x.
Savage KI, Matchett KB, Barros EM, Cooper KM, Irwin GW, Gorski JJ, et al. 2014. BRCA1 deficiency exacerbates estrogen-induced DNA damage and genomic instability. Cancer Res 74(10):2773–2784, PMID: 24638981, https://doi.org/10.1158/0008-5472.CAN-13-2611.
Schlotz N, Kim G-J, Jäger S, Günther S, Lamy E. 2017. In vitro observations and in silico predictions of xenoestrogen mixture effects in T47D-based receptor transactivation and proliferation assays. Toxicol In Vitro 45(Pt 1):146–157, PMID: 28855101, https://doi.org/10.1016/j.tiv.2017.08.017.
Schlumpf M, Cotton B, Conscience M, Haller V, Steinmann B, Lichtensteiger W. 2001. In vitro and in vivo estrogenicity of UV screens. Environ Health Perspect 109(3):239–244, PMID: 11333184, https://doi.org/10.1289/ehp.01109239.
Schlumpf M, Kypke K, Wittassek M, Angerer J, Mascher H, Mascher D, et al. 2010. Exposure patterns of UV filters, fragrances, parabens, phthalates, organochlor

pesticides, PBDEs, and PCBs in human milk: correlation of UV filters with use of cosmetics. Chemosphere 81(10):1171–1183, PMID: 21030064, https://doi.org/10.1016/j.chemosphere.2010.09.079.

Schock H, Zeleniuch-Jacquotte A, Lundin E, Grankvist K, Lakso HÅ, Idahl A, et al. 2016. Hormone concentrations throughout uncomplicated pregnancies: a longitudinal study. BMC Pregnancy Childbirth 16(1):146, PMID: 27377060, https://doi.org/10.1186/s12884-016-0937-5.

Scientific Committee on Consumer Products. 2005. Extended Opinion on the Safety Evaluation of Parabens. https://ec.europa.eu/health/ph_risk/committees/04_sccp/docs/sccp_o_019.pdf [accessed 11 August 2019].

Scientific Committee on Consumer Products. 2008. Opinion on benzophenone-3. https://ec.europa.eu/health/ph_risk/committees/04_sccp/docs/sccp_o_159.pdf [accessed 11 August 2019].

Shang Y, Hu X, DiRenzo J, Lazar MA, Brown M. 2000. Cofactor dynamics and sufficiency in estrogen receptor–regulated transcription. Cell 103(6):843–852, PMID: 11136970, https://doi.org/10.1016/s0092-8674(00)00188-4.

Shivji MKK, Renaudin X, Williams CH, Venkitaraman AR. 2018. BRCA2 regulates transcription elongation by RNA polymerase II to prevent R-loop accumulation. Cell Rep 22(4):1031–1039, PMID: 29386125, https://doi.org/10.1016/j.celrep.2017.12.086.

Snodin D. 2017. Regulatory risk assessments: is there a need to reduce uncertainty and enhance robustness? Update on propylparaben in relation to its EU regulatory status. Hum Exp Toxicol 36(10):1007–1014, PMID: 28695774, https://doi.org/10.1177/0960327117718042.

Sollier J, Stork C, García-Rubio ML, Paulsen RD, Aguilera A, Cimprich KA. 2014. Transcription-coupled nucleotide excision repair factors promote R-loop-induced genome instability. Mol Cell 56(6):777–785, PMID: 25435140, https://doi.org/10.1016/j.molcel.2014.10.020.

Soni MG, Burdock GA, Taylor SL, Greenberg NA. 2001. Safety assessment of propyl paraben: a review of the published literature. Food Chem Toxicol 39(6):513–532, PMID: 11346481, https://doi.org/10.1016/s0278-6915(00)00162-9.

Stork CT, Bocek M, Crossley MP, Sollier J, Sanz LA, Chédin F, et al. 2016. Co-transcriptional R-loops are the main cause of estrogen-induced DNA damage. eLife 5:e17548, PMID: 27552054, https://doi.org/10.7554/eLife.17548.

Tarazona I, Chisvert A, Salvador A. 2013. Determination of benzophenone-3 and its main metabolites in human serum by dispersive liquid–liquid microextraction followed by liquid chromatography tandem mass spectrometry. Talanta 116:388–395, PMID: 24148420, https://doi.org/10.1016/j.talanta.2013.05.075.

Tuduri S, Crabbé L, Conti C, Tourrière H, Holtgreve-Grez H, Jauch A, et al. 2009. Topoisomerase I suppresses genomic instability by preventing interference between replication and transcription. Nat Cell Biol 11(11):1315–1324, PMID: 19838172, https://doi.org/10.1038/ncb1984.

Vladusic EA, Hornby AE, Guerra-Vladusic FK, Lakins J, Lupu R. 2000. Expression and regulation of estrogen receptor beta in human breast tumors and cell lines. Oncol Rep 7(1):157–167, PMID: 10601611, https://doi.org/10.3892/or.7.1.157.

Wan Y, Zheng X, Chen H, Guo Y, Jiang H, He X, et al. 2015. Splicing function of mitotic regulators links R-loop–mediated DNA damage to tumor cell killing. J Cell Biol 209(2):235–246, PMID: 25918225, https://doi.org/10.1083/jcb.201409073.

Wang Z, Chandrasena ER, Yuan Y, Peng KW, van Breemen RB, Thatcher GR, et al. 2010. Redox cycling of catechol estrogens generating apurinic/apyrimidinic sites and 8-oxo-deoxyguanosine via reactive oxygen species differentiates equine and human estrogens. Chem Res Toxicol 23(8):1365–1373, PMID: 20509668, https://doi.org/10.1021/tx1001282.

Wang IX, Grunseich C, Fox J, Burdick J, Zhu Z, Ravazian N, et al. 2018. Human proteins that interact with RNA/DNA hybrids. Genome Res 28(9):1405–1414, PMID: 30108179, https://doi.org/10.1101/gr.237362.118.

Warth B, Raffeiner P, Granados A, Huan T, Fang M, Forsberg EM, et al. 2018. Metabolomics reveals that dietary xenoestrogens alter cellular metabolism induced by palbociclib/letrozole combination cancer therapy. Cell Chem Biol 25(3):291–300, PMID: 29337187, https://doi.org/10.1016/j.chembiol.2017.12.010.

Watanabe Y, Kojima H, Takeuchi S, Uramaru N, Sanoh S, Sugihara K, et al. 2015. Metabolism of UV-filter benzophenone-3 by rat and human liver microsomes and its effect on endocrine-disrupting activity. Toxicol Appl Pharmacol 282(2):119–128, PMID: 25528284, https://doi.org/10.1016/j.taap.2014.12.002.

Woodruff TJ, Zota AR, Schwartz JM. 2011. Environmental chemicals in pregnant women in the United States: NHANES 2003–2004. Environ Health Perspect 119(6):878–885, PMID: 21233055, https://doi.org/10.1289/ehp.1002727.

Xu X, Roman JM, Issaq HJ, Keefer LK, Veenstra TD, Ziegler RG. 2007. Quantitative measurement of endogenous estrogens and estrogen metabolites in human serum by liquid chromatography-tandem mass spectrometry. Anal Chem 79(20):7813–7821, PMID: 17848096, https://doi.org/10.1021/ac070494j.

Yager JD, Davidson NE. 2006. Estrogen carcinogenesis in breast cancer. N Engl J Med 354(3):270–282, PMID: 16421368, https://doi.org/10.1056/NEJMra050776.

Ye X, Bishop AM, Reidy JA, Needham LL, Calafat AM. 2006. Parabens as urinary biomarkers of exposure in humans. Environ Health Perspect 114(12):1843–1846, PMID: 17185273, https://doi.org/10.1289/ehp.9413.

Yi P, Wang Z, Feng Q, Chou C-K, Pintilie GD, Shen H, et al. 2017. Structural and functional impacts of ER coactivator sequential recruitment. Mol Cell 67(5):733–743, PMID: 28844863, https://doi.org/10.1016/j.molcel.2017.07.026.

Zhang X, Chiang H-C, Wang Y, Zhang C, Smith S, Zhao X, et al. 2017. Attenuation of RNA polymerase II pausing mitigates BRCA1-associated R-loop accumulation and tumorigenesis. Nat Commun 8:15908, PMID: 28649985, https://doi.org/10.1038/ncomms15908.

Zhao Z, Kosinska W, Khmelnitsky M, Cavalieri EL, Rogan EG, Chakravarti D, et al. 2006. Mutagenic activity of 4-hydroxyestradiol, but not 2-hydroxyestradiol, in BB rat2 embryonic cells, and the mutational spectrum of 4-hydroxyestradiol. Chem Res Toxicol 19(3):475–479, PMID: 16544955, https://doi.org/10.1021/tx0502645.

Zhao X, Malhotra GK, Lele SM, Lele MS, West WW, Eudy JD, et al. 2010. Telomerase-immortalized human mammary stem/progenitor cells with ability to self-renew and differentiate. Proc Natl Acad Sci USA 107(32):14146–14151, PMID: 20660721, https://doi.org/10.1073/pnas.1009030107.

Ziegler RG, Faupel-Badger JM, Sue LY, Fuhrman BJ, Falk RT, Boyd-Morin J, et al. 2010. A new approach to measuring estrogen exposure and metabolism in epidemiologic studies. J Steroid Biochem Mol Biol 121(3–5):538–545, PMID: 20382222, https://doi.org/10.1016/j.jsbmb.2010.03.068.